Vibrational Analysis of Conical Shells: Development of a Semi-Analytical Finite Element Method

Sean Tuinstra

Delft University of Technology

July 2024

Student number: -

Thesis committee:

Dr. ir. A. Tsouvalas,	TU Delft, Chair
Dr. ir. A. Tsetas,	TU Delft, Daily Supervisor
Ir. C. Kasbergen	TU Delft, Supervisor

Abstract

This thesis presents the development and validation of a Semi-Analytical Finite Element (SAFE) model for conical shells. The motivation behind this research is to provide a computationally efficient and accurate numerical model for analysing conical shells. Starting with general equations of motion, kinematic equations, constitutive equations, and boundary conditions, the SAFE method is used to construct a numerical framework for conical shells.

Validation of the SAFE method is performed through comparative analyses with a detailed COMSOL model. The comparison focuses on the natural frequencies, mode shapes, and responses to both uniform and non-uniform harmonic loading. The results demonstrate that the SAFE method achieves accurate predictions in all analyses.

To demonstrate the robustness of the SAFE model, the analysis is extended to include a coupled conical-cylindrical shell system. Similar analyses are performed, and the model continues to provide accurate predictions.

These findings highlight the capability of the SAFE method in delivering both computationally efficient and accurate solutions for the analysis of conical shells.

Preface

This thesis focuses on the development of a numerical framework for the analysis of conical shells using the Semi-Analytical Finite Element (SAFE) method. The motivation behind this work comes from the need for a more efficient approach to do analysis on conical shells.

As I near the end of this thesis, I realise I've learned as much about myself as about the topic. The beginning was particularly tough, starting on a subject with limited prior knowledge felt intimidating. The initial months involved a lot of work, and results were slow to appear. This was expected, but it was mentally challenging to stay motivated without seeing immediate outcomes. This experience taught me that even when results aren't immediate, persistence is key. Just keep going and believe in the process and it eventually leads to progress.

I would like to express my gratitude to my daily supervisor, Dr. Ir. A. Tsetas, whose extensive knowledge of implementing the SAFE method on shells was invaluable throughout this process. His guidance and support were instrumental in my work, and I am thankful for his help. I also extend my thanks to Dr. A. Tsouvalas and Ir. C. Kasbergen, who served as the chair supervisor and additional grader for this project, respectively. Their valuable feedback and assessment during the progress meetings were instrumental in guiding the development of this thesis and contributed to its successful completion.

Furthermore, I would like to thank my friends and family for their support during this challenging period in my academic career. A special thanks to Jerom, with whom I spent countless days making progress on our theses, as we were navigating similar challenges together. Also, my father and mother deserve attention, as they gave confidence in my abilities to finish this thesis.

Sean Tuinstra
Heemskerk, July 2024

Contents

Preface **1**

1 Introduction **3**
1.1 Research Objectives . . . 4
1.2 Research Questions . . . 4

2 Mathematical Foundations for the SAFE Method **7**

3 Semi-Analytical Finite Element (SAFE) Model for Conical Shells **11**

4 Model Setup in COMSOL **15**
4.1 Geometric Definitions . . . 15
4.2 Material Properties . . . 16
4.3 Loads . . . 16
4.4 Boundary Conditions . . . 17
4.5 Analyses . . . 17

5 Results and Analysis of the Conical Shell **20**
5.1 Free Vibration Analysis . . . 21
5.2 Comparison of Eigenmodes . . . 23
5.3 Types of loading . . . 25
5.3.1 Uniform Distributed load . . . 27
5.3.2 Triangular-Shaped Distributed load . . . 27
5.4 Static analysis . . . 28
5.4.1 Static Response of Conical Shell to Uniform Loading . . . 28
5.4.2 Static Response of Conical Shell to Triangular Loading . . . 29
5.5 Harmonic Response Analysis . . . 30
5.5.1 Harmonic Response of Conical Shell to Uniform Loading . . . 30
5.5.2 Harmonic Response of Conical Shell to Triangular Loading . . . 32

6 Results and Analysis of the Coupled Conical-Cylindrical Shell **38**
6.1 Free Vibration Analysis . . . 39
6.2 Comparison of Eigenmodes . . . 41
6.3 Static Analysis . . . 42
6.3.1 Static Response of Coupled Conical-Cylindrical Shell to Uniform Loading . . . 43
6.3.2 Static Response of Coupled Conical-Cylindrical Shell to Triangular Loading . . . 43
6.4 Harmonic Response Analysis . . . 43
6.4.1 Harmonic Response of Coupled Conical-Cylindrical Shell to Uniform Loading . . . 44
6.4.2 Harmonic Response of Coupled Conical-Cylindrical Shell to Triangular Loading . . . 45

7 Conclusion **49**

Chapter 1

Introduction

Conical shells are commonly used in various engineering applications, including aircraft, driving piles, submarines and storage tanks. In certain cases, for example driving piles or off-shore wind turbines, the dimensions can be very large. Due to these large dimensions, modelling these structures as cylindrical shells might not be appropriate. Instead, these structures would be better represented as coupled conical-cylindrical shell structures.

Existing methods, such as finite element software, already allow for modelling of these structures. In this method, the structure is divided into many small, more manageable elements, and in solving for each element and combining the solutions we can analyse the structure as a whole. However, analysing these structures with such software can be very tedious and time-consuming. Therefore, an alternative method is desired. The semi-analytical finite element (SAFE) method could be a suitable solution. By employing finite elements in the longitudinal direction of the shell and analytical functions in the circumferential direction, the SAFE method simplifies the problem from a 3D to a 2D problem, making computations easier and faster. The development of this numerical framework, would result in a tool that is, robust and easy to use, capable of accurately modelling these structures while being computationally efficient and still having high accuracy.

Shell structures are important in many engineering applications, so a lot of shell theories have already been developed based on different assumptions. These are comprehensively documented in Leissa [1]. While extensive research has been conducted on cylindrical shells, conical shells have received comparatively less attention. This is likely due to the increased complexity of conical shells, which arise from the varying radius along the longitudinal axis. This results in more complex equations, which makes finding solutions more challenging.

Even though it is a complex problem, Wu and Huang used the finite annular prism method to study stress and deformation of bi-directional functionally graded truncated conical shells[2]. Saunders, Wisniewski, and Paslay employed the Rayleigh-Ritz procedure to calculate the natural frequencies of the shell. They began by assuming mode shapes that satisfy the boundary conditions. By equating the maximum potential and kinetic energy, and then applying the Rayleigh-Ritz procedure to this equation, they were able to determine the natural frequencies.[3]. Garnet and Kempner investigated how incorporating transverse shear deformation and rotary inertia affects the axisymmetric free vibrations of a truncated conical shell. They employed the Rayleigh-Ritz procedure in their study[4]. Goldberg and Bogdanoff presented a numerical method for determining the axisymmetric modes of vibration and natural frequencies of thin conical shells. They made use of power series to obtain the displacement field of the shell [5]. Jin, Ma, Shi, Ye and Liu conducted a free vibration analysis of truncated conical shell with general elastic boundary conditions. They improved the displacement function by using a standard Fourier series and introducing some auxiliary functions to ensure and accelerate the convergence of the series expansion. They also applied the Rayleigh-Ritz method[6]. Guo presented a theoretical study on waves in conical shells, discussing in detail the propagation of the waves toward the apex of the shell[7]. Ni and Elliot used a wave finite element (WFE) to study the types of waves in a conical shell. They developed a method to decompose the overall response of a numerical model into its wave components[8]. Shu used the Generalized Differential Quadrature to study the free vibrations of the isotropic conical shells. By discretising the boundary conditions and governing equations, the natural frequencies of the system can easily and accurately be obtained. The method is examined by comparing the results to results in the literature and close agreement is found[9]. Raju, Venkateswara Rao, Prakasa Rao and Venkataramana developed a curved conical shell element, designed to exactly fit in the geometry of conical shells[10].

As mentioned earlier, the semi-analytical finite element (SAFE) method could be applicable in this case. This method combines analytical functions with finite elements. In the case of conical shells, the circumference can be represented using sine or cosine functions, as these functions repeat periodically after one revolution, matching the shell's geometry. The shell can be divided longitudinally into finite elements, and the displacement at each node can be calculated. By using interpolation between the nodes and the analytical functions in the circumferential direction, the entire displacement field of the shell can be represented. This assumed displacement field can then be used in the SAFE method.

Many engineering challenges can be simplified using the SAFE method. For example, the SAFE method has been used in developing a method for modelling the propagation of lamb waves in homogeneous and isotropic composite plates[11]. It has also been applied to investigate the guided wave properties of anisotropic composite laminates with varying plate thickness[12]. Additionally, the structural response of asphalt pavement to static loads was obtained by using the SAFE method with the solution verified through the software ABAQUS. [13]. Furthermore, Ramesh and Ganesan developed a semi-analytical finite element specifically for analysing the free vibrations of multi-layered composite conical shells. Their approach, based on discrete-layer theory, produced results consistent with existing literature across various boundary conditions[14].

1.1 Research Objectives

The primary objectives of this thesis are outlined as follows:

1. **Development of the SAFE Method:** The primary objective of this thesis is to develop a robust numerical framework using the semi-analytical finite element (SAFE) method for the accurate modeling of conical shells.

2. **Validation of the SAFE Method:** The second objective is to validate the accuracy and efficiency of the SAFE method by comparing its results with those obtained from the finite element software COMSOL.

3. **Coupling Conical and Cylindrical Shells:** The third objective is to model and analyse the coupling between conical and cylindrical shells, ensuring that the combined shell structure can be accurately represented and analysed with the SAFE framework.

1.2 Research Questions

1. **How can we make a numerical framework for conical shells?**

   The approach to answer this question is to use the available data for cylindrical shells and apply this knowledge to the method for conical shells. Warburton used Flügge's three equations of motion for uniform thin cylindrical shells to derive a general solution, from which the dependence between the natural frequencies and the dimensions of the cylindrical shell could be investigated for different boundary conditions [15]. Callahan proposed a closed-form solution procedure for circular cylindrical shell vibrations. The eigensolution could be obtained without knowing the absolute dimensions or material properties [16]. Ovesy and Fazitah employed the semi-analytical finite strip method to perform a stability analysis of cylindrical shell structures [17]. Alijani, Darvizeh, and Anzouri developed a semi-analytical nonlinear finite element method for cylindrical shells according to a continuum-based approach. They used the semi-analytical finite element method for cylindrical shells with and without imperfections and two types of perturbations, load and displacement based, to find the post-buckling behavior of the shell [18].

   The cylindrical shell can be viewed as a specific case of a conical shell with an inclination of 0 degrees. While both cylindrical and conical shells are governed by similar equations of motion, the equations of motion for conical shells include additional terms which are dependent on the angle of inclination.

   To develop the kinematic equations, the relationship between displacements and strains is defined. Next, the relationship between the strains and the forces needs to be defined to obtain the constitutive equations.

   By applying the balance of forces in the shell, the equations of motion are derived. Since the forces can be expressed as a function of the displacements, the equations of motion can be formulated to

be a function of the displacements. With the displacement field being fully defined, as explained earlier using the SAFE method, the problem can be solved.

After specifying the boundary conditions, the principle of virtual work is applied to obtain the mass and stiffness matrix for a conical shell element. Finally, by assembling these matrices, we construct a global mass and stiffness matrix, which represent the whole conical shell.

2. **How can the SAFE method be validated?**

   Once the global mass and stiffness matrices are constructed, several analyses will be performed to validate the SAFE method:

   First, an eigenvalue analysis to determine the natural frequencies and the corresponding mode shapes of the conical shell. These will be compared to those from a model created using COMSOL Multiphysics [19]. This model will serve as the benchmark for validation of the applied semi-analytical finite element method.

   To further validate the SAFE method, a forced vibration study will be conducted. The whole forced vibration study is done for two types of loading: a uniform distributed load and a triangular shaped load. A force will be applied to the edge of the conical shell and a harmonic response analysis will be performed across a range of forcing frequencies. The response from the SAFE method will be compared to the solution from COMSOL to ensure that the SAFE method gives accurate solutions. Before conducting the dynamic analysis, an initial analysis will be carried out with a forcing frequency of 0 rad/s. This is done to ensure the reliability of the SAFE method by confirming that the system produces valid solutions under static conditions before continuing to the more advanced dynamic analysis. Additionally, this initial analysis will test the system's capability to handle boundary conditions. Following this, the conical shell will be subjected to loading across a range of forcing frequencies. In this way, a comprehensive dynamic analysis under external excitation is conducted. Results are compared to the dynamic response solutions obtained in COMSOL to verify that the SAFE model computes reliable results.

   This approach aims to provide a comprehensive validation of the SAFE method for conical shells.

3. **How will the coupling be done for the SAFE method?**

   Another aspect of the study will be to investigate the coupling between a conical shell and a cylindrical shell. If successful, this would demonstrate the robustness and versatility of the numerical framework. It will illustrate that the SAFE method can be used to create a conical shell element that can be used as easily as a 1D element, allowing for coupling with various other elements.

   Some research has already been done on the coupling of conical shells with cylindrical shells. Bagheri, Kiani, and Eslami studied the free vibrations of joined cylindrical-conical shells using the transfer matrix approach, in which the transfer matrix was expressed as a power series. They also studied the free vibrations of joined conical-cylindrical-conical shells using the first-order shear deformation shell theory (FSDT) of Mindlin [20][21]. Irie, Yamuda, and Muramoto also used the transfer matrix method to study the free vibrations of joined conical-cylindrical shells, varying the cone angle between -45 degrees and +45 degrees [22]. Caresta and Kessissoglou investigated the free vibrational characteristics of isotropic coupled cylindrical-conical shells. They used different methods for each part: a wave solution for the cylindrical shell and a power series for the conical shell. The coupling of the shells was performed using interface conditions [23]. Rezaiee-Pajand, Sobhani, and Masoudi performed a semi-analytical vibrational analysis on functionally graded carbon nanotubes modeled as coupled conical-conical structures. They used the first-order shear deformation theory and the Hamilton method to obtain the equations of motion and solved them by using the Generalized Differential Quadrature Method (GDQM) [24].

   The coupling of a conical shell and a cylindrical shell can be achieved elegantly using the SAFE framework for conical shells. Since the stiffness and mass matrices depend on the inclination angle α, setting α to zero gives the matrices for the cylindrical shell. These stiffness and mass matrices are assembled in the global stiffness matrix.

   It is crucial to ensure that these matrices are correctly rotated before assembling them. This is because these matrices are calculated based on displacements aligned with the local axes of the shell. Since the local axes of the conical shell are differently orientated, than for the cylindrical shell, the element stiffness and mass matrices must be rotated into the global coordinate system before being

assembled into the global mass and stiffness matrices. In this way, the coupled conical-cylindrical shell is modeled.

To assess the complex geometry, the same analyses that were performed on the conical shell are also performed on the coupled conical-cylindrical shell.

Chapter Overview

In this thesis, the Semi-Analytical Finite Element (SAFE) method is used to construct a numerical framework for conical shells. Chapter 2 presents the mathematical foundation necessary for implementing the SAFE method, including the equations of motion, kinematic and constitutive equations, and boundary conditions. Chapter 3 will focus on implementing the SAFE method, building on the mathematical foundation. Chapter 4 presents the model made in COMSOL to use as a benchmark for the validation of the SAFE method. In Chapter 5, the results from the SAFE method will be shown and compared to the COMSOL model. Chapter 6 presents a method for coupling the conical elements to cylindrical elements to construct coupled conical-cylindrical shells, which is validated in this chapter. The thesis will be closed with Chapter 7, the conclusion.

Chapter 2

Mathematical Foundations for the SAFE Method

In this section, the mathematical steps for general shells are outlined. With the classical theory of small displacement of thin shells the following assumptions were made by Love[1]:

- The thickness is very small compared to the other dimensions in the shell.
- Strains and displacements are so small, the first-order terms are so dominant, that the second- and higher-order terms can be neglected.
- The transverse normal stress is small compared to the other normal stresses and so this is also neglected.
- The normals to the undeformed middle surface remain straight and normal to the deformed middle surface and are not subjected to extension.

In order to satisfy the fourth assumptions, referred to as Kirchhoff's hypothesis:

$$\gamma_{\alpha z} = 0 \tag{2.1a}$$
$$\gamma_{\beta z} = 0 \tag{2.1b}$$
$$e_z = 0 \tag{2.1c}$$

The displacements are restricted to these linear relations:

$$U(\alpha, \beta, z) = u(\alpha, \beta) + z\theta_\alpha(\alpha, \beta) \tag{2.2}$$
$$V(\alpha, \beta, z) = v(\alpha, \beta) + z\theta_\beta(\alpha, \beta) \tag{2.3}$$
$$W(\alpha, \beta, z) = w(\alpha, \beta) \tag{2.4}$$

In which u, v and w are displacements at the middle of the shell surface, z is the coordinate along the thickness of the shell. θ_α and θ_β are the rotations of the normal to the middle of the surface given in equations 2.5 and 2.6:

$$\theta_\alpha = \frac{u}{R_\alpha} - \frac{1}{A}\frac{\partial w}{\partial \alpha} \tag{2.5}$$
$$\theta_\beta = \frac{v}{R_\beta} - \frac{1}{B}\frac{\partial w}{\partial \beta} \tag{2.6}$$

The shell theory that will be considered, is the Love-Timoshenko theory for thin shells. The strains along the thickness of the shell are represented through the following equations:

$$e_\alpha = \epsilon_\alpha + z\kappa_\alpha \tag{2.7a}$$
$$e_\beta = \epsilon_\beta + z\kappa_\beta \tag{2.7b}$$
$$\gamma_{\alpha\beta} = \epsilon_{\alpha\beta} + z\tau \tag{2.7c}$$

The terms ϵ_α, ϵ_β, $\epsilon_{\alpha\beta}$, κ_α, κ_β and τ for the Love-Timoshenko theory are defined by:

$$\epsilon_\alpha = \frac{1}{A}\frac{\partial u}{\partial \alpha} + \frac{v}{AB}\frac{\partial A}{\partial \beta} + \frac{w}{R_\alpha} \tag{2.8a}$$

$$\epsilon_\beta = \frac{u}{AB}\frac{\partial B}{\partial \alpha} + \frac{1}{B}\frac{\partial v}{\partial \beta} + \frac{w}{R_\beta} \tag{2.8b}$$

$$\epsilon_{\alpha\beta} = \frac{A}{B}\frac{\partial}{\partial \beta}\left(\frac{u}{A}\right) + \frac{B}{A}\frac{\partial}{\partial \alpha}\left(\frac{v}{B}\right) \tag{2.8c}$$

$$\kappa_\alpha = \frac{1}{A}\frac{\partial \theta_\alpha}{\partial \alpha} + \frac{\theta_\beta}{AB}\frac{\partial A}{\partial \beta} \tag{2.8d}$$

$$\kappa_\beta = \frac{\theta_\alpha}{AB}\frac{\partial B}{\partial \alpha} + \frac{1}{B}\frac{\partial \theta_\beta}{\partial \beta} \tag{2.8e}$$

$$\begin{aligned}\tau = {} & \frac{A}{B}\frac{\partial}{\partial \beta}\left(\frac{\theta_\alpha}{A}\right) + \frac{B}{A}\frac{\partial}{\partial \alpha}\left(\frac{\theta_\beta}{B}\right) \\ & + \frac{1}{R_\alpha}\left(\frac{1}{B}\frac{\partial u}{\partial \beta} - \frac{v}{AB}\frac{\partial B}{\partial \alpha}\right) \\ & + \frac{1}{R_\beta}\left(\frac{1}{A}\frac{\partial v}{\partial \alpha} - \frac{u}{AB}\frac{\partial B}{\partial \beta}\right)\end{aligned} \tag{3.8f}$$

After obtaining the strain-displacement relations, we proceed to the strain-stress relations, which are given by Hooke's law. With Kirchhoff's hypothesis, only the following relations are non-zero:

$$e_\alpha = \frac{1}{E}(\sigma_\alpha - \nu\sigma_\beta) \tag{2.9a}$$

$$e_\beta = \frac{1}{E}(\sigma_\beta - \nu\sigma_\alpha) \tag{2.9b}$$

$$\gamma_{\alpha\beta} = \frac{2(1+\nu)}{E}\sigma_{\alpha\beta} \tag{2.9c}$$

These formulas relate the stress to the strain in the shell, with Young's modulus E and the Poisson's ratio ν.

By inverting the strain-stress relations, the stress-strain relations are obtained:

$$\sigma_\alpha = \frac{E}{1-\nu^2}(e_\alpha + \nu e_\beta) \tag{2.10a}$$

$$\sigma_\beta = \frac{E}{1-\nu^2}(e_\beta + \nu e_\alpha) \tag{2.10b}$$

$$\sigma_{\alpha\beta} = \frac{E}{2(1+\nu)}\gamma_{\alpha_\beta} \tag{2.10c}$$

These stress equations are integrated over the thickness of the shell. For a thin shell, it is assumed that the bending radius is very large compared to the shell's thickness. Consequently, when the stress equations are integrated to obtain the forces, the resulting expressions include a linear term in the thickness:

$$N_\alpha = \frac{Eh}{1-\nu^2}(\epsilon_\alpha + \nu\epsilon_\beta) \tag{2.11a}$$

$$N_\beta = \frac{Eh}{1-\nu^2}(\epsilon_\beta + \nu\epsilon_\alpha) \tag{2.11b}$$

$$N_{\alpha\beta} = \frac{Eh}{2(1+\nu)}\epsilon_{\alpha\beta} \tag{2.11c}$$

$$M_\alpha = \frac{Eh^3}{12(1-\nu^2)}(\kappa_\alpha + \nu\kappa_\beta) \tag{2.11d}$$

$$M_\beta = \frac{Eh^3}{12(1-\nu^2)}(\kappa_\beta + \nu\kappa_\alpha) \tag{2.11e}$$

$$M_{\alpha\beta} = \frac{Eh^3}{24(1+\nu)}\tau \tag{2.11f}$$

The equilibrium equations are derived by considering equilibrium of the shell. This results in three force equilibrium equations corresponding to the three directions: along α, along β, and normal to these two directions. Additionally, moment equilibrium must be satisfied, leading to two more equilibrium equations for moments.

These are the general equations of motion for shells, where α, β, A and B vary depending on the type of shell. The resulting general force equilibrium equations are:

$$\frac{\partial}{\partial\alpha}(BN_\alpha) + \frac{\partial}{\partial\beta}(AN_{\beta\alpha}) + \frac{\partial A}{\partial\beta}N_{\alpha\beta} - \frac{\partial B}{\partial\alpha}N_\beta + \frac{AB}{R_\alpha}Q_\alpha + ABq_\alpha = 0 \tag{2.12}$$

$$\frac{\partial}{\partial\beta}(AN_\beta) + \frac{\partial}{\partial\alpha}(BN_{\alpha\beta}) + \frac{\partial B}{\partial\alpha}N_{\beta\alpha} - \frac{\partial A}{\partial\beta}N_\beta + \frac{AB}{R_\beta}Q_\beta + ABq_\beta = 0 \tag{2.13}$$

$$-\frac{B}{R_\alpha}N_\alpha - \frac{AB}{R_\beta}N_\beta + \frac{\partial}{\partial\alpha}(BQ_\alpha) + \frac{\partial}{\partial\beta}(AQ_\beta) + ABq_n = 0 \tag{2.14}$$

And the resulting general moment equilibrium equations are:

$$\frac{\partial}{\partial\alpha}(BM_\alpha) + \frac{\partial}{\partial\beta}(AM_{\beta\alpha}) + \frac{\partial A}{\partial\beta}M_{\alpha\beta} - \frac{\partial B}{\partial\alpha}M_\beta - ABQ_\alpha + ABm_\beta = 0 \tag{2.15}$$

$$\frac{\partial}{\partial\beta}(AM_\beta) + \frac{\partial}{\partial\alpha}(BM_{\alpha\beta}) + \frac{\partial B}{\partial\alpha}M_{\beta\alpha} - \frac{\partial A}{\partial\beta}M_\beta - ABQ_\beta + ABm_\alpha = 0 \tag{2.16}$$

These are the general equations for shells. Now, let us consider the specific case of conical shells. For conical shells, the fundamental parameters are defined as follows, based on Leissa's Section 5.1:

$$\begin{aligned} \alpha &= s, \qquad \beta = \theta \\ A &= 1, \qquad B = R = s\sin\alpha \\ R_\alpha &= \infty, \quad R_\beta = r = s\tan\alpha \end{aligned} \tag{2.17}$$

The inertia that will be considered in the equations of motion are given by:

$$\begin{aligned} q_\alpha &= -\rho h\frac{\partial^2 u}{\partial t^2} \\ q_\beta &= -\rho h\frac{\partial^2 v}{\partial t^2} \\ q_n &= -\rho h\frac{\partial^2 w}{\partial t^2} \end{aligned} \tag{2.18}$$

These fundamental parameters for conical shells are substituted into the general equations of motion, resulting in the specific equations of motion for conical shells:

$$\frac{\partial N_s}{\partial s} + \frac{1}{s\sin\alpha}\frac{\partial N_{s\theta}}{\partial\theta} + \frac{N_s}{s} - \frac{N_\theta}{s} = \rho h\frac{\partial^2 u}{\partial t^2} \tag{2.19a}$$

$$\frac{1}{s\sin\alpha}\frac{\partial N_\theta}{\partial\theta} + \frac{\partial N_{s\theta}}{\partial s} + \frac{N_{s\theta}}{s} + \frac{N_{\theta s}}{s} + \frac{Q_\theta}{s\tan\alpha} = \rho h\frac{\partial^2 v}{\partial t^2} \tag{2.19b}$$

$$\frac{\partial Q_s}{\partial s} + \frac{1}{s\sin\alpha}\frac{\partial Q_\theta}{\partial \theta} - \frac{N_\theta}{s\sin\alpha} + \frac{Q_s}{s} = \rho h \frac{\partial^2 w}{\partial t^2} \tag{2.19c}$$

$$\frac{\partial M_s}{\partial s} + \frac{1}{s\sin\alpha}\frac{\partial M_{\theta s}}{\partial \theta} + \frac{M_s}{s} + \frac{M_\theta}{s} - Q_s = 0 \tag{2.19d}$$

$$\frac{1}{s\sin\alpha}\frac{\partial M_\theta}{\partial \theta} + \frac{\partial M_{s\theta}}{\partial s} + \frac{M_{s\theta}}{s} + \frac{M_{\theta s}}{s} - Q_\theta = 0 \tag{2.19e}$$

These are the equations that will be used in the SAFE method. Before implementing this method, it is necessary to consider the boundary conditions. In this thesis, free boundaries are considered, and the following relations are applicable in this case:

$$N_s = 0 \tag{2.20a}$$

$$N_{s\theta} + \frac{M_{s\theta}}{R_\theta} = 0 \tag{2.20b}$$

$$Q_s + \frac{1}{s\sin\alpha}\frac{\partial M_{s\theta}}{\partial \theta} = 0 \tag{2.20c}$$

$$M_s = 0 \tag{2.20d}$$

In this section, the equations of motion, kinematic equations, constitutive equations, and boundary conditions for the conical shell have been presented. These equations and relations establish the essential foundation for implementing the Semi-Analytical Finite Element (SAFE) method. With these fundamentals in place, the next step will be to apply the SAFE method to develop the numerical framework and analysis.

These equations shown here including: equations of motion, the kinematic equations, the constitutive equations and the boundary conditions, are the ground for the development of the numerical framework and these will be the foundation for the implementation of the SAFE method in the next chapter.

Chapter 3

Semi-Analytical Finite Element (SAFE) Model for Conical Shells

In this section, the implementation of the Semi-Analytical Finite Element (SAFE) method for constructing a numerical framework for conical shells will be discussed. This formulation builds upon the equations derived in the previous chapter, including the equations of motion, kinematic and constitutive equations, and boundary conditions. We will start with the equations of motion, which can be expressed in the following matrix form:

$$\mathbf{p}_p + \mathbf{L}_p \mathbf{s}_p - \mathbf{I}_p \mathbf{A}_p \frac{\partial^2 \mathbf{u}_p}{\partial t^2} = \mathbf{0} \tag{3.1}$$

Where $\mathbf{u}_p$ is the displacement vector $\mathbf{p}_p$ is the external force vector. Specifically,

$$\mathbf{u}_p = \begin{bmatrix} u_p & v_p & w_p & \beta_s \end{bmatrix}^T \tag{3.2}$$

$$\mathbf{p}_p = \begin{bmatrix} p_{s,p} & p_{\theta,p} & p_{r,p} & m_{s,p} & m_{\theta,p} \end{bmatrix}^T \tag{3.3}$$

The internal force vector is represented as $\mathbf{s}_p$. It is calculated using the differential operators $\mathbf{S}_p$ and $\mathbf{A}_p$. The vector $\mathbf{s}_p$ is given by:

$$\mathbf{s}_p = \mathbf{S}_p \mathbf{A}_p \mathbf{u}_p = \begin{bmatrix} N_s & N_\theta & N_{s\theta} & N_{\theta s} & Q_s & Q_\theta & M_s & M_\theta & M_{s\theta} & M_{\theta s} \end{bmatrix}^T \tag{3.4}$$

To obtain the correct formulation of the matrix form for the equations of motion, several differential operators are introduced:

- $\mathbf{S}_p$: This operator relates the internal forces to the displacements. It is given by:

$$\mathbf{S}_p(\cdot) = \mathbf{S}_{0,p}(\cdot) + \mathbf{S}_{s,p}\frac{\partial(\cdot)}{\partial s} + \mathbf{S}_{\theta,p}\frac{\partial(\cdot)}{\partial \theta} + \mathbf{S}_{ss,p}\frac{\partial^2(\cdot)}{\partial s^2} + \mathbf{S}_{\theta\theta,p}\frac{\partial^2(\cdot)}{\partial \theta^2} + \mathbf{S}_{s\theta,p}\frac{\partial^2(\cdot)}{\partial s \partial \theta} \tag{3.5}$$

- $\mathbf{L}_p$: This operator is used to construct the correct equations of motion by performing the necessary derivatives of the force vector. It is given by:

$$\mathbf{L}_p(\cdot) = \mathbf{L}_{s,p}\frac{\partial(\cdot)}{\partial s} + \mathbf{L}_{\theta,p}\frac{\partial(\cdot)}{\partial \theta} + \mathbf{L}_{0,p}(\cdot) \tag{3.6}$$

- $\mathbf{A}_p$: This operator is used to determine the full displacement vector. Since β_θ is a function of the other displacements, the full displacement vector $\mathbf{u}_p$ can be written in terms of $\mathbf{u}_p$. It is given by:

$$\mathbf{A}_p(\cdot) = \mathbf{A}_{0,p}(\cdot) + \mathbf{A}_{\theta,p}\frac{\partial(\cdot)}{\partial \theta} \tag{3.7}$$

The full displacement vector is calculated as:

$$\mathbf{a}_p = \mathbf{A}_p \mathbf{u}_p = \begin{bmatrix} u_p & v_p & w_p & \beta_s & \beta_\theta \end{bmatrix}^T \tag{3.8}$$

The tractions at both the left and right boundaries of the conical shell element can be described as follows:

$$\mathbf{t}_p^{(L)} = -(\mathbf{B}_p \mathbf{s}_p)^{(L)} \tag{3.9a}$$

$$\mathbf{t}_p^{(R)} = (\mathbf{B}_p \mathbf{s}_p)^{(R)} \tag{3.9b}$$

In these formulations, the matrix $\mathbf{B}_p$ operates on the internal force vector $\mathbf{s}_p$ to obtain the tractions at the boundaries of a conical shell element:

$$\mathbf{B}_p \mathbf{s}_p = \begin{bmatrix} N_s & N_{s\theta} + \dfrac{M_{s\theta}}{s \cdot \tan\alpha} & Q_s + \dfrac{1}{s \sin\alpha} \dfrac{\partial M_{s\theta}}{\partial \theta} & M_s \end{bmatrix}^T \tag{3.10}$$

The matrix $\mathbf{B}_p$ is constructed as:

$$\mathbf{B}_p = \mathbf{B}_{0,p}(\cdot) + \mathbf{B}_{\theta,p} \frac{\partial(\cdot)}{\partial \theta} \tag{3.11}$$

$$\mathbf{t}_p = \begin{bmatrix} t_{s,p} & t_{\theta,p} & t_{r,p} & t_{ss,p} \end{bmatrix}^T \tag{3.12}$$

In this equation, the traction vector components are shown, including forces and moments in all relevant directions: normal, radial, circumferential, and rotational.

The SAFE model will be formulated by discretising the shell in the s direction and using the analytical functions for the circumferential direction. The displacement vector of a conical shell element will have the following form:

$$\mathbf{u}_p = \mathbf{\Theta}_n \mathbf{N}_p \mathbf{x}_p \tag{3.13}$$

with the nodal displacement vector:

$$\mathbf{x}_p = \begin{bmatrix} \mathbf{x}_p^{(L)} \\ \mathbf{x}_p^{(R)} \end{bmatrix} \tag{3.14}$$

In this displacement vector, the displacement field can be expressed as a function of the nodal displacements by using the interpolation matrix $\mathbf{N}_p$ and the matrix $\mathbf{\Theta}_n$.

The displacement along the circumference is modelled by the matrix $\mathbf{\Theta}_n$, which includes the analytical functions of θ. There are two types of motion considered: symmetrical and asymmetrical. The following matrices illustrate these relationships for each type of motion.

$$\mathbf{\Theta}_n^s = \begin{bmatrix} \cos(n\theta) & 0 & 0 & 0 \\ 0 & -\sin(n\theta) & 0 & 0 \\ 0 & 0 & \cos(n\theta) & 0 \\ 0 & 0 & 0 & \cos(n\theta) \end{bmatrix} \tag{3.15a}$$

$$\mathbf{\Theta}_n^a = \begin{bmatrix} \sin(n\theta) & 0 & 0 & 0 \\ 0 & \cos(n\theta) & 0 & 0 \\ 0 & 0 & \sin(n\theta) & 0 \\ 0 & 0 & 0 & \sin(n\theta) \end{bmatrix} \tag{3.15b}$$

The interpolation matrix contains the functions used to interpolate the four displacements between two nodes. Linear interpolation is applied to u and v displacements, while cubic interpolation is used for the w and β_s. The length of the conical shell element is represented by d_l, which is defined along the inclined axis of the shell. The interpolation matrix reads:

$$\mathbf{N}_p = \begin{bmatrix} N_1^l(s) & 0 & 0 & 0 & N_2^l(s) & 0 & 0 & 0 \\ 0 & N_1^l(s) & 0 & 0 & 0 & N_2^l(s) & 0 & 0 \\ 0 & 0 & N_1^c(s) & -N_2^c(s) & 0 & 0 & N_3^c(s) & -N_4^c(s) \\ 0 & 0 & -\dfrac{dN_1^c(s)}{ds} & \dfrac{dN_2^c(s)}{ds} & 0 & 0 & -\dfrac{dN_3^c(s)}{ds} & \dfrac{dN_4^c(s)}{ds} \end{bmatrix}$$

The linear interpolation funcions for u and v:

$$N_1^l = \frac{s_2 - s}{d_l} \tag{3.16a}$$

$$N_2^l = \frac{s}{d_l} \tag{3.16b}$$

And the cubic interpolation functions for w and β_s:

$$N_1^c = 1 - \frac{3s^2}{d_l^2} + \frac{2s^2}{d_l^3} \tag{3.17a}$$

$$N_2^c = s - \frac{2s^2}{d_l} + \frac{s^3}{d_l^2} \tag{3.17b}$$

$$N_3^c = \frac{3s^2}{d_l^2} - \frac{2s^2}{d_l^3} \tag{3.17c}$$

$$N_4^c = -\frac{s^2}{d_l} + \frac{s^3}{d_l^2} \tag{3.17d}$$

With all definitions in place, the principle of virtual work is formulated for the conical shell elements. This principle leads to the following formulation:

$$\int_0^{2\pi} (\delta \mathbf{u}_p^{(L)})^T \mathbf{r}_p^{(L)} r(s_1)\, d\theta \; + \int_0^{2\pi} (\delta \mathbf{u}_p^{(R)})^T \mathbf{r}_p^{(R)} r(s_2)\, d\theta \; + \int_{s_1}^{s_2} \int_0^{2\pi} \delta \mathbf{a}_p^T \mathbf{r}_{p,V} r(s)\, d\theta \; ds = 0 \tag{3.18}$$

As can be seen in the equation, three terms are present. The first two terms represent the residual forces on the left and right boundaries of the shell segment. The third term represents the residual internal forces. According to the principle of virtual work, the sum of these residual forces when multiplied with a virtual displacement should equal zero.

The residual forces at the boundaries are defined as:

$$\mathbf{r}_p^{(L)} = \mathbf{t}_p^{(L)} + (\mathbf{B}_p \mathbf{s}_p)^{(L)} \tag{3.19a}$$

$$\mathbf{r}_p^{(R)} = \mathbf{t}_p^{(R)} - (\mathbf{B}_p \mathbf{s}_p)^{(R)} \tag{3.19b}$$

In the same manner, the residual internal forces are described by:

$$\mathbf{r}_{p,V} = \mathbf{p}_p + \mathbf{L}_p \mathbf{s}_p - \mathbf{I}_p \mathbf{A}_p \frac{\partial^2 \mathbf{u}_p}{\partial t^2} \tag{3.20}$$

In the absence of external forces and surface tractions, and by substituting the above formulations, the new virtual work equation simplifies to:

$$\int_0^{2\pi} -(\delta \mathbf{u}_p^T \mathbf{B}_p \mathbf{s}_p r)|_{s_2}^{s_1}\, d\theta \; + \int_{s_1}^{s_2} \int_0^{2\pi} \delta \mathbf{a}_p^T \left(\mathbf{L}_p \mathbf{s}_p - \mathbf{I}_p A_p \frac{\partial^2 \mathbf{u}_p}{\partial t^2} \right) r(s)\, d\theta \; ds = 0 \tag{3.21}$$

The term corresponding to the boundary terms can be rewritten as a surface integral, this gives:

$$\begin{aligned} \int_0^{2\pi} \int_{s_1}^{s_2} -\left(\frac{\mathrm{d}(\delta \mathbf{u}_p^T)}{\mathrm{d}s} \mathbf{B}_p \mathbf{s}_p r_p \right) - \left(\delta \mathbf{u}_p^T \frac{\mathrm{d}(\mathbf{B}_p \mathbf{s}_p)}{\mathrm{d}s} r(s) \right) - \left(\delta \mathbf{u}_p^T \mathbf{B}_p \mathbf{s}_p \frac{\mathrm{d}(r(s))}{\mathrm{d}s} \right) \mathrm{d}s\, \mathrm{d}\theta \\ + \int_0^{2\pi} \int_{s_1}^{s_2} (\delta \mathbf{a}_p)^T \left(\mathbf{L}_p \mathbf{s}_p - \mathbf{I}_p \mathbf{A}_p \frac{\mathrm{d}^2 \mathbf{u}_p}{\mathrm{d}t^2} \right) r(s)\, \mathrm{d}s\, \mathrm{d}\theta = 0 \end{aligned} \tag{3.22}$$

For the virtual work principle, it is known that it holds for any arbitrary virtual displacement. Therefore, by factoring the virtual displacement vector from the equation, we obtain the following result:

$$\int_0^{2\pi}\int_{s_1}^{s_2}\Bigg((\mathbf{N}_n^\theta)^T\frac{\mathrm{d}(\mathbf{B}_p\mathbf{S}_p\mathbf{A}_p\mathbf{N}_n^\theta)}{\mathrm{d}s}r(s)+\frac{\mathrm{d}(\mathbf{N}_n^\theta)^T}{\mathrm{d}s}\mathbf{B}_p\mathbf{S}_p\mathbf{A}_p\mathbf{N}_n^\theta r(s)$$

$$+(\mathbf{N}_n^\theta)^T\mathbf{B}_p\mathbf{S}_p\mathbf{A}_p\mathbf{N}_n^\theta\frac{\mathrm{d}r(s)}{\mathrm{d}s}-(\mathbf{N}_n^\theta)^T\mathbf{A}_p^T\mathbf{L}_p\mathbf{S}_p\mathbf{A}_p\mathbf{N}_n^\theta r(s)\Bigg)\,\mathrm{d}s\,\mathrm{d}\theta\,\mathbf{x}_p \tag{3.23}$$

$$+\int_0^{2\pi}\int_{s_1}^{s_2}\Big((\mathbf{N}_n^\theta)^T\mathbf{A}_p^T\mathbf{I}_p\mathbf{A}_p\mathbf{N}_n^\theta r(s)\Big)\,\mathrm{d}s\,\mathrm{d}\theta\,\frac{\mathrm{d}^2\mathbf{x}_p}{\mathrm{d}t^2}=0$$

In this equation $r(s)$ represents the radius of the cone at the coordinate s, not to be confused with the formulas for residual forces $\mathbf{r}_p$. Finally, it can be seen that in the formulation now a term is present with no time dependency, and a term present with time dependency. These correspond to the stiffness and mass matrix respectively. These are presented here:

$$\mathbf{M}_n^{elem}=\int_0^{2\pi}\int_{s_1}^{s_2}\Big((\mathbf{N}_n^\theta)^T\mathbf{A}_p^T\mathbf{I}_p\mathbf{A}_p\mathbf{N}_n^\theta r(s)\Big)\,\mathrm{d}s\,\mathrm{d}\theta \tag{3.24}$$

$$\begin{aligned}\mathbf{K}_n^{elem}=\int_0^{2\pi}\int_{s_1}^{s_2}\Bigg[&(\mathbf{N}_n^\theta)^T\frac{\mathrm{d}(\mathbf{B}_p\mathbf{S}_p\mathbf{A}_p\mathbf{N}_n^\theta)}{\mathrm{d}s}\,r(s)\\&+\frac{\mathrm{d}(\mathbf{N}_n^\theta)^T}{\mathrm{d}s}\mathbf{B}_p\mathbf{S}_p\mathbf{A}_p\mathbf{N}_n^\theta\,r(s)\\&+(\mathbf{N}_n^\theta)^T\mathbf{B}_p\mathbf{S}_p\mathbf{A}_p\mathbf{N}_n^\theta\frac{\mathrm{d}r(s)}{\mathrm{d}s}\\&-(\mathbf{N}_n^\theta)^T\mathbf{A}_p^T\mathbf{L}_p\mathbf{S}_p\mathbf{A}_p\mathbf{N}_n^\theta\,r(s)\Bigg]\,\mathrm{d}s\,\mathrm{d}\theta\end{aligned} \tag{3.25}$$

Remarks SAFE method

In the SAFE method, the element mass and stiffness matrices inlude the term $\mathbf{N}_n^\theta$. This is done for brevity, this term is defined as $\mathbf{N}_n^\theta=\mathbf{N}_p\mathbf{\Theta}_n$.

After deriving the mathematical expressions for the element stiffness and mass matrices of the conical shell, the next step involved implementing these expressions in Maple and solving them. Initially, attempts were made to express all variables analytically. However, this approach encountered challenges during the integration process aimed at obtaining the mass and stiffness matrices. To address these challenges, two strategies were employed.

The first strategy involved initialising the terms with an original radius R_1 and setting the variable s to start from this point. This allowed the angle α to be set to zero, simplifying the conical shell element to a cylindrical shell element.

Secondly, an approximation strategy utilizing Taylor expansion was implemented. For instance, expressions of the form $\dfrac{1}{R_1+s\cdot\sin(\alpha)}$ led to complex equations when combined with other terms, resulting in impractical outcomes. By approximating these functions terms, using Taylor expansion, it produced a more manageable expression. For example, $\dfrac{1}{R_1+s\cdot\sin(\alpha)}$, would become: $\dfrac{1}{R_1}-\dfrac{\sin(\alpha)}{R_1^2}s+\dfrac{\sin^2(\alpha)}{R_1^3}s^2$.

These two strategies led to simpler equations that were more easily solvable. The results of this approach will be tested extensively in the thesis.

Chapter 4

Model Setup in COMSOL

This section presents the setup and configuration of two models in COMSOL Multiphysics. The first model represents a conical shell, and the second model represents a coupled conical-cylindrical shell. Detailed descriptions of the geometries, material properties, boundary conditions, meshing, and settings for the eigenvalue analysis and forced vibration analysis are provided.

4.1 Geometric Definitions

Model 1: Conical Shell

The conical shell geometry was created using the primitives section under the Geometry tab in COMSOL. For this model, the cone option was selected with the type set to Surface. The resulting geometry is an open truncated conical shell with the following specifications:

- **Left Radius:** 0.8 meters
- **Right Radius:** 3 meters
- **Horizontal Length:** 10 meters
- **Cone Angle (α):** 12.4 degrees
- **Shell Thickness:** 0.0159 meters

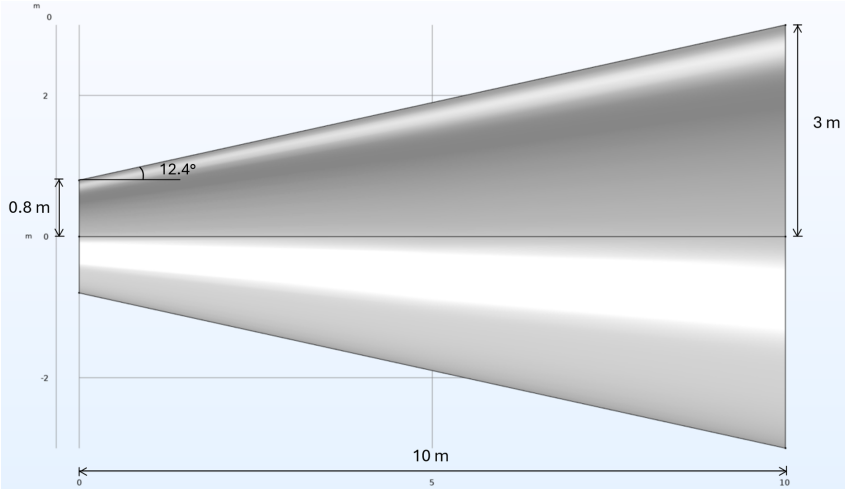

Figure 4.1: Geometry of conical shell in COMSOL

Model 2: Coupled Conical-Cylindrical Shell

The coupled conical-cylindrical shell geometry was constructed by combining a conical section with a cylindrical section, which are automatically connected in COMSOL. The specifications for each section are as follows:

Conical Shell Section

- **Left Radius:** 0.8 meters
- **Right Radius:** 3 meters
- **Horizontal Length:** 5 meters
- **Cone Angle:** 27.4 degrees

Cylindrical Shell Section

- **Radius:** 3 meters
- **Horizontal Length:** 5 meters
- **Shell Thickness:** 0.0159 meters

This geometry is presented in the figure below:

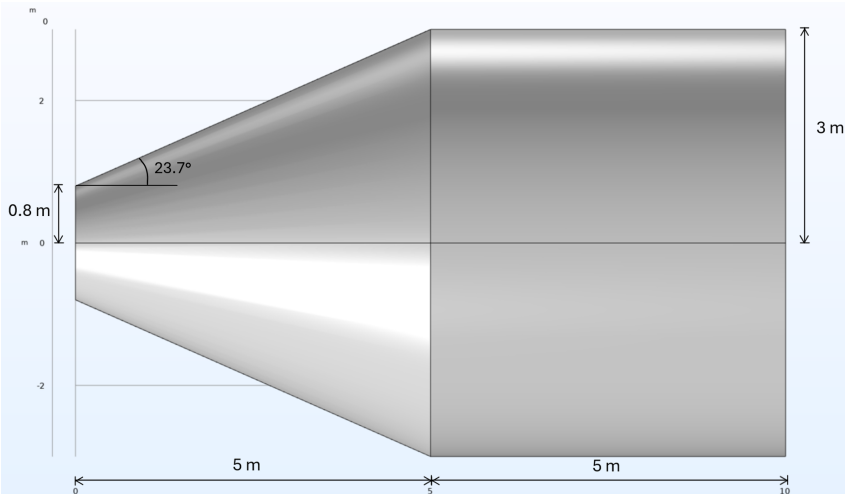

Figure 4.2: Geometry of coupled conical-cylindrical shell in COMSOL

4.2 Material Properties

The material of the shell is chosen to be steel with the following properties:

- **Density:** 7850 kg/m^3
- **Poisson's Ratio:** 0.3
- **Young's Modulus:** 210 GPa

These properties are applied to both the conical shell and the coupled conical-cylindrical shell.

4.3 Loads

To perform a comprehensive vibrational analysis, two types of loads will be considered:

- **Uniform Distributed Load:** This load is applied uniformly along the circumference of the boundary.
- **Triangular-Shaped Distributed Load:** This load has a triangular distribution along the circumference of the boundary.

These loads are illustrated in Figure 4.3. The horizontal axis represents the angular coordinate along the circumference of the boundary where the force is applied. Both types of loads will be used in the static force analysis and the forced vibration analysis.

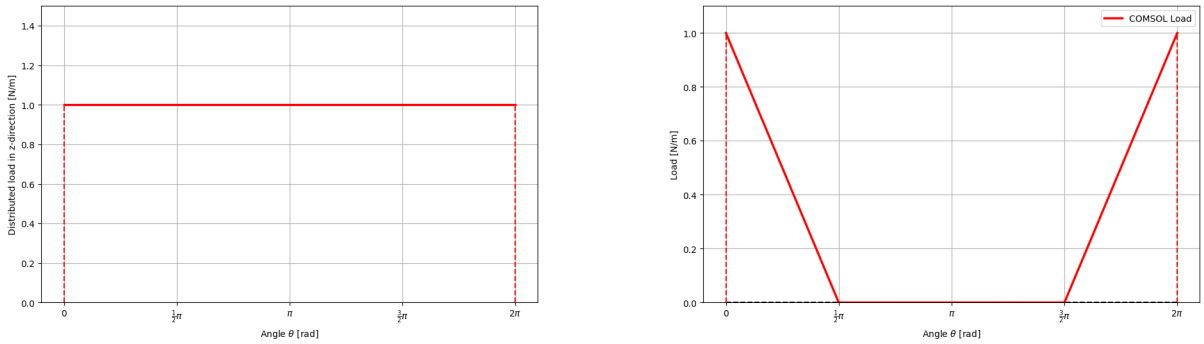

(a) Uniform load

(b) Triangular load

Figure 4.3: Loading Types

4.4 Boundary Conditions

The analyses involve different types of boundary conditions applied at the edges of geometries. These boundary conditions are categorised as either free or clamped:

- **Free Boundary Condition:** This condition implies that there are no restrictions on any displacements at the boundary. Points along a free edge of the shell are free to displace in any direction.
- **Clamped Boundary Condition:** Under this condition, all displacements at the boundary are constrained to zero. This means that no displacements are possible at the clamped edges, effectively fixing the boundary in place.

Mesh specification

The mesh used in all analyses consists of quadratic quadrilateral elements with a maximum size of 0.1 meters. Due to the inclination of the conical shell, the elements may not fit perfectly into an exact multiple of 0.1 meters. As a result, the elements could be slightly smaller. However, the maximum element size of 0.1 meters is used to describe the mesh size.

Damping

To ensure a meaningful comparison between the results from the COMSOL model the SAFE method, damping is introduced in both systems. Damping serves to stabilise the systems by preventing unbounded responses that occur in undamped systems.

Hysteretic damping is used; in COMSOL this is implemented by specifying an isotropic structural loss factor, denoted as η_s. this factor is defined by:

$$\eta_s = 2\xi\omega \tag{4.1}$$

where ξ represents the damping ratio, and ω is the angular frequency of the system in rad/s. The damping specified in this section is used in the forced vibration study.

4.5 Analyses

To validate the SAFE method against the COMSOL model, a series of analyses will be conducted. Initially, a free vibration analysis to determine the natural frequencies and corresponding eigenmodes. Following this, a static force analysis will be conducted to verify the system's expected behavior under

static load. Finally, a forced vibration analysis will assess the systems's response to different forcing frequencies. By comparing the results from these COMSOL analyses to the solutions obtained using the SAFE method, the accuracy and validity of the SAFE method can be evaluated. In this section all of these analyses will be described how these are conducted in COMSOL:

Free Vibration Analysis

The free vibration analysis is performed on both the conical shell and the coupled shell to obtain the natural frequencies. Important parameters for the free vibration analysis are given:

- **Boundary conditions**: Free-free boundary conditions.
- **Mesh size**: Maximum element size of 0.1 meters.
- **Procedure**: Use the "Eigenfrequency" study in COMSOL to determine the eigenmodes. 1000 eigenfrequencies are computed for the conical shell, and 2000 for the coupled conical-cylindrical shell.
- **Output**: Natural frequencies and eigenmodes
- **Post-processing**: Compare the obtained natural frequencies with those obtained from the SAFE method.

Static Load Analysis

Before proceeding to dynamic analysis, it is important to verify that the SAFE method accurately predicts the response to static loads and handles boundary conditions correctly. This verification will be conducted in this analysis by applying a force at the left boundary of both the conical shell and the coupled conical-cylindrical shell.

Important parameters for the static load analysis include:

- **Forcing Frequency**: 0 Hz (static load implies no change in force over time, resulting in a constant displacement solution).
- **Loading**: Uniform distributed load and triangular-shaped distributed load.
- **Boundary Conditions**: Free-clamped boundary conditions (to ensure deterministic structural behavior under static load).
- **Mesh Size**: Maximum element size of 0.1 meters.
- **Procedure**: Use the "Frequency Domain" study in COMSOL to perform the static analysis.
- **Output**: Forced response.
- **Post-processing**: Compare the obtained forced responses with those obtained from the SAFE method.

Forced Vibration Analysis

After completing the static analysis, a forced vibration analysis will be conducted on both the conical shell and the coupled conical-cylindrical shell. This analysis involves calculating the structural response to each frequency step. Important parameters for the forced vibration analysis are given below:

- **Forcing Frequency Range**: 1 Hz to 300 Hz, with steps of 1 Hz.
- **Loading**: Uniform distributed load and triangular-shaped distributed load.
- **Boundary Conditions**: Free-free boundary conditions
- **Damping**: Hysteretic damping with $\xi = 0.01$ is incorporated to stabilise the analysis.
- **Mesh Size**: Maximum element size of 0.1 meters.

- **Procedure**: Use the "Frequency Domain" study in COMSOL to perform a harmonic response analysis.
- **Output**: Forced responses.
- **Post-processing**: Compare the obtained forced responses with those obtained from the SAFE method.

Additional Consideration

To ensure the reliability of the results obtained from COMSOL, a verification was performed to check the sensitivity of the mesh size, tested up to a forcing frequency of 300 Hz. It was observed that increasing the mesh density beyond the maximum element size of 0.1 meters did not significantly improve the results. This indicates that the chosen mesh size is sufficient and the results can be considered valid.

Chapter 5

Results and Analysis of the Conical Shell

This section presents the results obtained using the Semi-analytical Finite Element (SAFE) method for a truncated conical shell and compares these results with those from COMSOL Multiphyics, a widely used, finite-element software. Several analyses are conducted, starting with the free vibration analysis. The analysis of free vibrations in a structure is important for understanding its dynamic behavior. Free vibration analysis enables the prediction of natural frequencies and mode shapes, which are unique per structure. By identifying the frequencies at which the structure tends to vibrate, and the corresponding deformation patterns, this analysis provides valuable insights into how the structure will respond to dynamic loading.

Therefore, it is crucial that the SAFE method accurately captures these characteristics. This analysis aims to demonstrate the SAFE method's capability in obtaining natural frequencies and mode shapes. The validation of these results will be done by comparing them with those from COMSOL. It is aimed to show the capacity of the SAFE method, for producing accurate results in a fraction of the time used compared to COMSOL.

After obtaining and comparing the dynamic characteristics from the free vibration analysis, the next step in the validation process is to conduct a dynamic analysis. This analysis will allow to evaluate the SAFE method on its performance on obtaining forced responses. By performing these analyses, we ensure that the SAFE method can accurately determine the vibrational behavior of conical shells.

In this analysis, the COMSOL mesh was refined to elements with a maximum element size of 0.1m. It was observed that increasing the mesh density beyond the maximum element size of 0.1 meters did not significantly improve the results. This indicates that the chosen mesh size is sufficient and the results can be considered valid.

The geometrical and material properties are once again shown in table 5.1.

Geometrical Properties	**Value**	**Units [m]**
Radius left	0.8	m
Radius right	3.0	m
Length	10.0	m
Material Properties	**Value**	**Unit**
Density (ρ)	7850	kg/m^3
Poisson's ratio (ν)	0.3	-
Thickness (h)	0.0159	m
Young's modulus (E)	210	GPa

Table 5.1: Geometrical and Material Properties of the Conical Shell

In the following sections, each analysis will be explained in detail, followed by the presentation of the results.

It is important to note that all results presented in the analyses are evaluated at $\theta = 0$ for symmetrical motion. At this angle, only axial and radial displacements of the conical shell are displayed because tangential displacements are zero at $\theta = 0$. This approach is used to provide clearer presentation of the results.

5.1 Free Vibration Analysis

The global stiffness and mass matrix of the conical shell are obtained by assembling the element stiffness and mass matrices obtained in the chapter SAFE. By setting the force to zero and substituting the assumed solution for the displacements we get to the eigenvalue problem:

$$(-\omega_{nj}^2 \mathbf{M}_n + \mathbf{K}_n)\mathbf{u}_{nj} = \mathbf{0} \tag{5.1}$$

Solutions $\mathbf{u}_{nj}$ of these eigenvalue problem contain $U_{nj}(s)$, $V_{nj}(s)$, $W_{nj}(s)$ and $\beta_{nj}(s)$.
The displacement of the shell can be written displacement in this form:

$$u(s,\theta,t) = \cos(n\theta)U_{nj}(s)\mathrm{e}^{i\omega_{nj}t} \tag{5.2a}$$

$$v(s,\theta,t) = \sin(n\theta)V_{nj}(s)\mathrm{e}^{i\omega_{nj}t} \tag{5.2b}$$

$$w(s,\theta,t) = \cos(n\theta)W_{nj}(s)\mathrm{e}^{i\omega_{nj}t} \tag{5.2c}$$

In the chapter SAFE, it was demonstrated that two solutions exist, referring to symmetric and asymmetric motion. These are obtained by swapping the functions sine and cosine, both are valid.

For axisymmetric ($n = 0$) motion, it can be observed that in the symmetric case, the system decouples the displacements U and W from V. By interchanging the cosine for sine function, the asymmetric case is obtained. Then when $n = 0$, it can be seen that only V has a non-zero value. This is referred to as the torsional mode.

It can be observed that there are two cases for the assumed solution. Namely the axisymmetric case ($n = 0$) motion and the non-axisymmetric motions ($n > 0$). In the case of $n > 0$, it can be observed that the displacements are all coupled. Therefore doing a free vibration analysis for both of these possibilities shows that all cases of vibration can be obtained using the SAFE method.

Solving this problem will result in natural frequencies and eigenmodes. The natural frequencies obtained from the SAFE method are then compared with those from the COMSOL model and these results will be reported. The analysis focuses on assessing the agreement between the natural frequencies derived from the SAFE method and those from COMSOL.

In the free vibration study, the boundary conditions are set to free-free. In the SAFE model, this condition is applied by having no changes done to the global stiffness and mass matrix. In the chapter on SAFE is explained how these boundary conditions are incorporated.

First, the axisymmetric modes, with $n = 0$, will be studied. Following this, non-axisymmetric modes with $n > 0$, will be studied. Doing these two analyses demonstrates that the model can both be used for axisymmetric and non-axisymmetric motions.

Axisymmteric Modes $n = 0$

First, a quick convergence study will be presented for the axisymmetric modes using the SAFE method. The natural frequencies of the SAFE model will be calculated for three different mesh sizes. Initially, a SAFE mesh with an element size of 0.2 meters will be used. This will be followed by testing a mesh with an element size of 0.1 meters, and finally, a mesh with an element size of 0.05 meters. The results will be analysed to evaluate convergence.

For comparison, the maximum element size used in the COMSOL model will be 0.1 meters. The result is shown in Figure 5.1

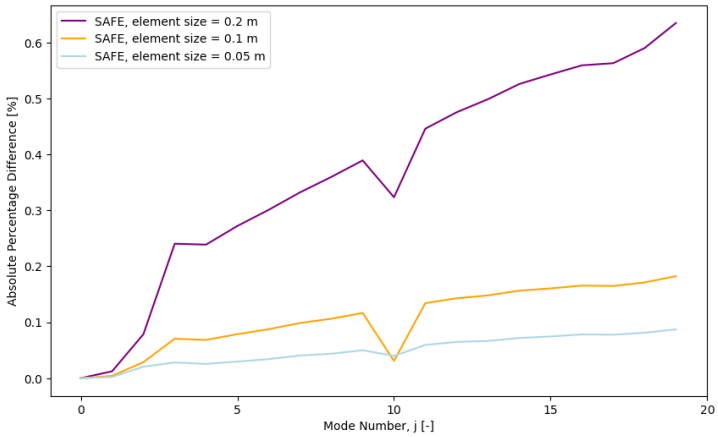

Figure 5.1: Convergence of SAFE Method for $n = 0$ modes

In Figure 5.1, it can be observed that the natural frequencies calculated by the SAFE method are in close agreement with those calculated by COMSOL. Even for a relatively coarse mesh with an element size of 0.2m in the SAFE model, the differences in natural frequencies for higher modes are small. Additionally, it can be observed that when the mesh from SAFE is refined, that the values go closer to the solutions from COMSOL. Indicating a stable solution from the SAFE method.

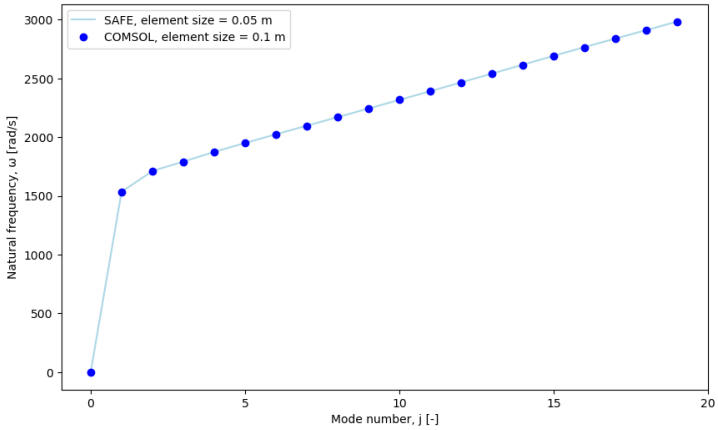

Figure 5.2: Comparison of Natural Frequencies Between Comsol and SAFE Method for $n = 0$ modes

In figure 5.2 the natural frequencies of both the COMSOL model and the SAFE method are plotted for $n = 0$ modes.

Non-Axisymmetric Modes $n = 1$

The same convergence analysis is performed on the non-axisymmetric modes with $n = 1$.

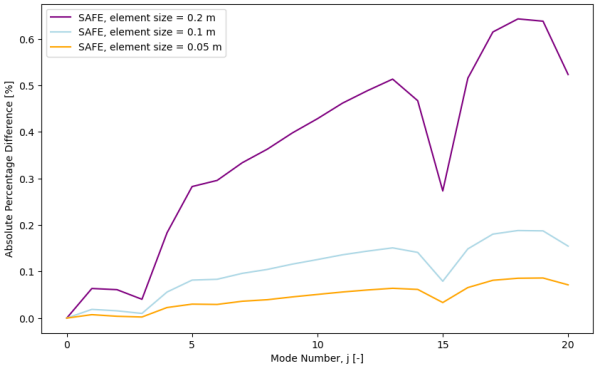

Figure 5.3: Convergence of SAFE Method for $n = 1$ modes

In Figure 5.1, again convergence is observed, for a refinement of SAFE mesh.

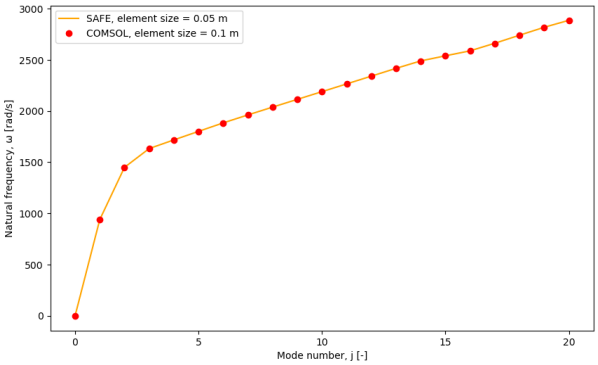

Figure 5.4: Comparison of Natural Frequencies Between Comsol and SAFE Method for $n = 1$ modes

In figure 5.4 the natural frequencies of both the COMSOL model and the SAFE method are plotted for $n = 1$ modes.

Overall, in both figures 5.2 and 5.4 it can be observed that the eigenfrequencies found from the SAFE method are very close to those found using the COMSOL model. This gives confidence that the SAFE model is working as expected. The fact that the SAFE method is accurately capturing both axisymmetric and non-axisymmetric motion gives great confidence in the validity of the SAFE method. For further validation, the eigenmodes that are linked to the found natural frequencies are inspected.

The table below presents the time required to complete the free vibration analyses using both methods. For the COMSOL model, the analysis involved calculating the first thousand eigenmodes, which took a total of 61 minutes. This corresponds to approximately 1 eigenmode every 3.6 seconds. In contrast, the SAFE method, during its 0.2 second analysis, was able to compute 603 eigenmodes, which comes out to approximately 0.00033 seconds per eigenmode. This substantial difference in computation time highlights the efficiency of the SAFE method for analysing conical shells.

	SAFE	**COMSOL**
Elements	200	19776
DoF	804	476928
Time	0.2 s	61 min
Time per mode	0.0003 s	3.6 s

Table 5.2: Comparison of Computational Resources and Time for SAFE and COMSOL

5.2 Comparison of Eigenmodes

The previous section showed that the eigenfrequencies obtained from the SAFE method closely match those from the COMSOL model. However, this provides only insight in one aspect of the dynamic

behavior of the system. The validation continues with finding the corresponding mode shapes. The mode shapes for both the axisymmetric ($n = 0$) and a non-axisymmetric ($n = 1$) case will be shown in this section.

Eigenmodes $n = 0$

First, starting with the modes with $n = 0$. These are presented in the following figure.

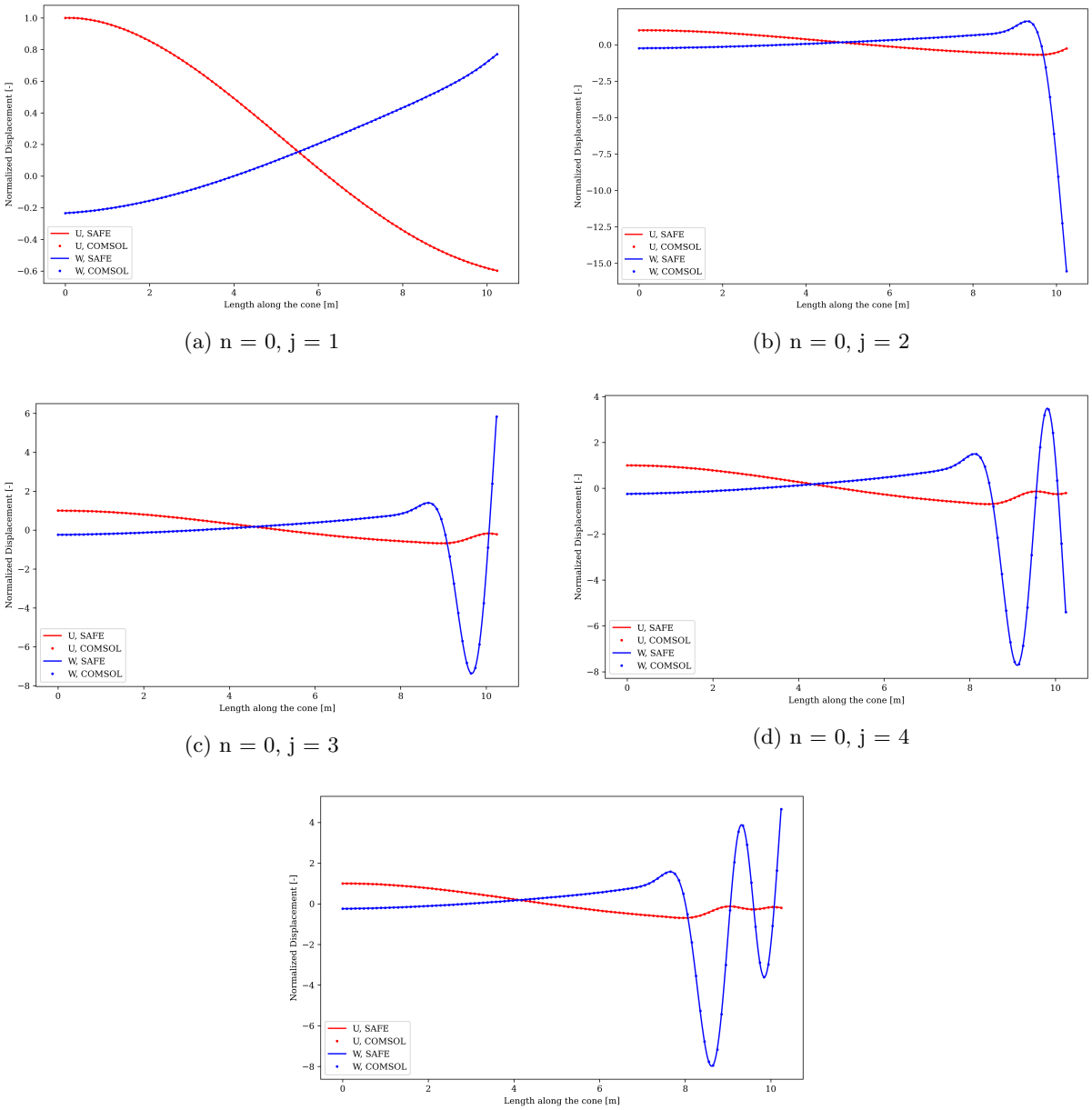

(a) n = 0, j = 1

(b) n = 0, j = 2

(c) n = 0, j = 3

(d) n = 0, j = 4

(e) n = 0, j = 5

Figure 5.5: Mode Shapes Conical shell, n = 0

In figure 5.5 the mode shapes are plotted for the first five modes with $n = 0$. The red line represents the U displacements, which are along the shell axis while the blue line indicates the W displacements which are perpendicular to the shell. The displacements for both methods are normalised by dividing the displacements by the U displacement at the left boundary.

A great similarity of the mode shapes can be observed between the SAFE method and the COMSOL model. This consistency in both the natural frequencies and the mode shapes demonstrates that the SAFE Method is able to accurately model axisymmetric motions.

Eigenmodes $n = 1$

In the same way now modes with $n = 1$ are inspected:

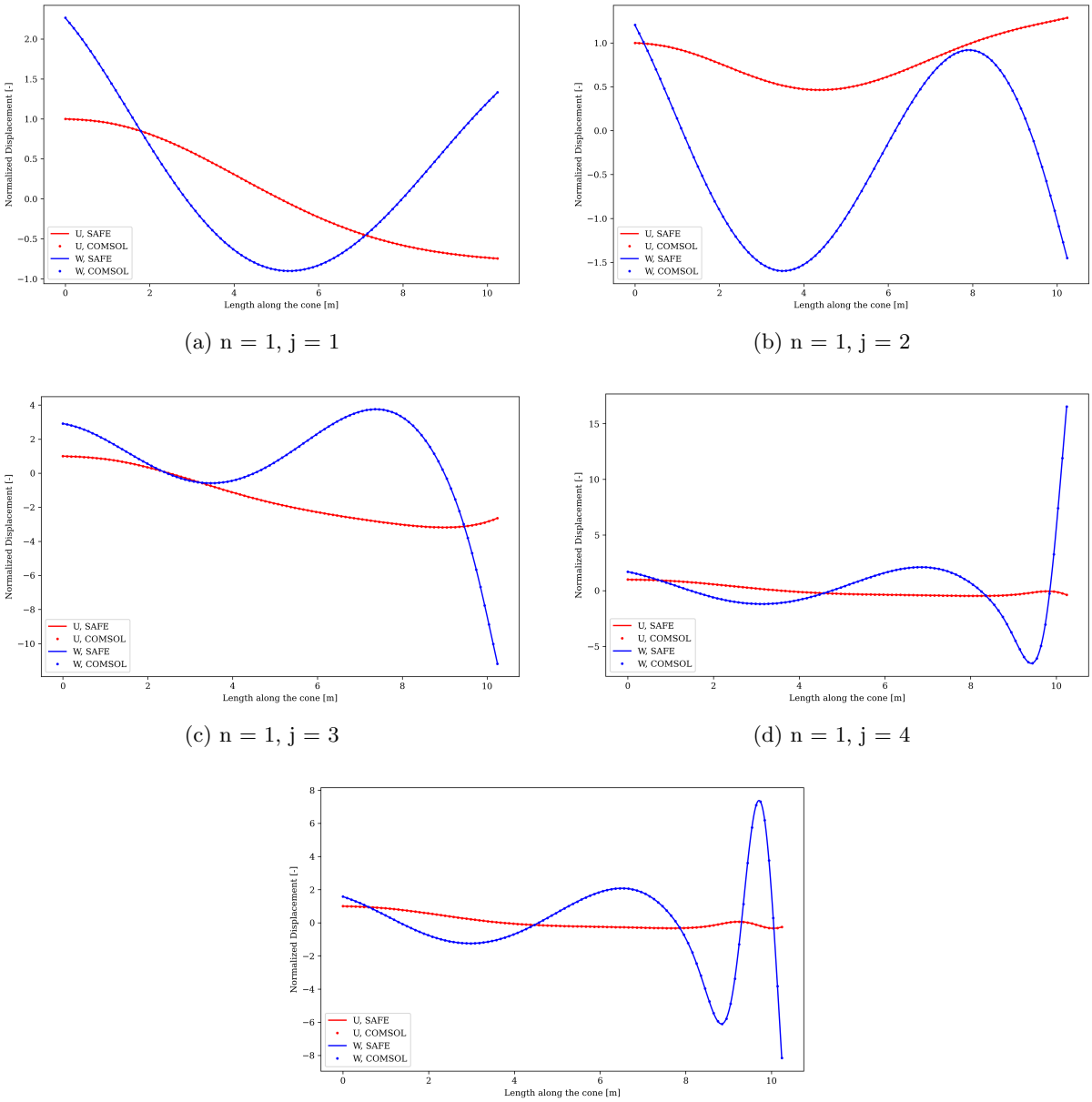

(a) n = 1, j = 1

(b) n = 1, j = 2

(c) n = 1, j = 3

(d) n = 1, j = 4

(e) n = 1, j = 5

Figure 5.6: Mode shapes for Conical shell, n = 1

In figure 5.6, mode shapes for the first five modes with $n = 1$ are presented. Similar to $n = 0$ modes, the U and W displacements are normalised and both methods again show great resemblance. The consistency in accurately capturing both axisymmetric and non-axisymmetric vibrational modes using the SAFE method indicates its robust performance. This consistency gives good confidence to proceed with the validation, now incorporating applied forces in the analysis.

5.3 Types of loading

To further validate the accuracy and capability of the SAFE method, a forced vibration analysis of the conical shell will be conducted. This analysis involves subjecting the conical shell to external harmonic forces to obtain the harmonic responses. This is an important step for validating the SAFE method. By comparing the results obtained from the SAFE method to those obtained from COMSOL, it ensures

that the SAFE method can not only capture the natural frequencies and the mode shapes but also the ability do accurately determine the response to loading.

In this analysis, hysteretic damping is used, to show that the SAFE method can incorporate damping effects and which make the comparison between the SAFE method and the COMSOL model more consistent.

In the application of forces using the SAFE method, certain calculations are required. Depending on the type of loading, multiple modes can be excited simultaneously. To determine the response of the SAFE method, distinct factors for exciting different modes must be identified. The next section explains how to calculate these factors.

From the SAFE method derivation, the force at the boundary can be written as:

$$\mathbf{p}_n = \int_0^{2\pi} \begin{bmatrix} \mathbf{\Theta}_n^T \mathbf{t}_p^{(L)} \\ \mathbf{\Theta}_n^T \mathbf{t}_p^{(R)} \end{bmatrix} R_p d\theta \tag{5.3}$$

The matrix $\mathbf{\Theta}_n^T$ defined in chapter 4 SAFE. The traction $\mathbf{t}_p^{(L)}$ can be written in the following form:

$$\mathbf{t}_p^{(L)} = \begin{bmatrix} p_s \\ p_\theta \\ p_r \\ m_{s,p} \end{bmatrix} f(\theta) \tag{5.4}$$

In this vector, the forcing amplitude is multiplied with a spacial function representing the loading distribution along the circumference of the boundary. This function can be expressed in a general formula, $f(\theta)$ defined as:

$$f(\theta) = \sum_{n=0}^{N} \left[f_n^s \cos(n\theta) + f_n^a \sin(n\theta) \right] \tag{5.5}$$

In this equation, the coefficients f_n^s and f_n^a are present to formulate the distribution of the load around the circumference. To arrive at a general formula for calculating the forcing coefficients f_n^s and f_n^a, a case for the radial forcing for the symmetric system is considered. Using equation 5.3 this results in the following integral:

$$\int_0^{2\pi} \cos(m\theta) \cdot p_r \cdot f(\theta) \cdot R_p^{(L)} d\theta = p_r R_p^{(L)} \int_0^{2\pi} \cos(m\theta) \left(\sum_{n=0}^{N} \left[f_n^s \cos(n\theta) + f_n^a \sin(n\theta) \right] \right) d\theta \tag{5.6}$$

It can be observed that only when $m = n$, there is a solution. This results in the next formula:

$$\int_0^{2\pi} \cos(m\theta) \cdot f(\theta) d\theta = f_n^s \int_0^{2\pi} \cos^2(n\theta) d\theta \tag{5.7}$$

Using the trigonometric identity:

$$\cos^2(\theta) = \frac{1}{2} + \frac{1}{2}\cos(2\theta) \tag{5.8}$$

This can be substituted into the previous equation and this gives:

$$\int_0^{2\pi} \cos(m\theta) \cdot f(\theta) d\theta = f_n^s \int_0^{2\pi} \left(\frac{1}{2} + \frac{1}{2}\cos(2n\theta) \right) d\theta \tag{5.9}$$

The integral of a periodic function over the domain from 0 to 2π returns 0. So the equation becomes:

$$\int_0^{2\pi} \cos(m\theta) \cdot f(\theta) d\theta = f_n^s \int_0^{2\pi} \frac{1}{2} d\theta \tag{5.10}$$

Then after evaluating the integral:

$$\int_0^{2\pi} \cos(m\theta) \cdot f(\theta) d\theta = f_n^s \pi \tag{5.11}$$

And finally we arrive at:

$$f_n^s = \int_0^{2\pi} \cos(m\theta) \cdot f(\theta) d\theta / \pi \tag{5.12}$$

This procedure is repeated for asymmetric case and these are the resulting equations:

$$m = n = 0: \quad f_0^s = \frac{1}{2\pi} \int_0^{2\pi} f(\theta)\, d\theta \tag{5.13a}$$

$$m = n = 0: \quad f_0^a = 0 \tag{5.13b}$$

$$m = n \neq 0: \quad f_n^s = \frac{1}{\pi} \int_0^{2\pi} \cos(m\theta) f(\theta)\, d\theta \tag{5.13c}$$

$$m = n \neq 0: \quad f_n^a = \frac{1}{\pi} \int_0^{2\pi} \sin(m\theta) f(\theta)\, d\theta \tag{5.13d}$$

The resulting equations are formulas for determining the coefficients that represent the distribution of loading along the circumference of the boundaries. The formulas above were derived by considering the force in the radial direction. These coefficients are used to represent all load distributions.

For the analyses, the force is applied in the horizontal direction. The displacements in the shell are defined along the axis of the shell and perpendicular to the shell. This means that the force needs to be projected onto these local axes. This is a straightforward calculation that involves rotating the force vector with an angle α.

5.3.1 Uniform Distributed load

The above functions can be used to find the coefficients representing the uniform distributed load. Since the load in this case, is the same for all theta along the circumference, this gives the function: $f(\theta) = 1$.

Using the above formulas for the coefficients in 5.13, it can be observed that only f_0^s has a non-zero value. So only $n = 0$ modes will be activated when the load is uniform. The calculation of the response to this type of load is therefore straightforward. Only one equation needs to be solved to determine the response.

5.3.2 Triangular-Shaped Distributed load

The functions used to determine the coefficients are also applicable to non-uniform loading patterns. In the case of the triangular-shaped distributed load, the distribution can be mathematically represented as follows:

$$f(\theta) = \begin{cases} 1 - \frac{2\theta}{\pi} & \text{if } \theta \in [0, \frac{1}{2}\pi], \\ 0 & \text{if } \theta \in [\frac{1}{2}\pi, 1\frac{1}{2}\pi], \\ \frac{2\theta - 3\pi}{\pi} & \text{if } \theta \in [1\frac{1}{2}\pi, 2\pi] \end{cases} \tag{5.14}$$

This triangular load is the same as the triangular load discussed in Chapter 5 for the COMSOL model. The load is symmetric around $\theta = 0$. Therefore, only symmetric coefficients will be non-zero.

This case was deliberately chosen to demonstrate the potential of this method in the simplest manner. Validating the approach for this load will be sufficient, as an asymmetric load will follow the same approach but require more calculations. Therefore, a symmetric load was considered here to keep the calculations straightforward and clear.

Using the formulas to obtain the first ten coefficients for the triangular load results in the following table:

Coefficient	Value (exact)	Value (decimal)
f_0^s	$\frac{1}{4}$	0.25
f_1^s	$\frac{4}{\pi^2}$	0.405
f_2^s	$\frac{2}{\pi^2}$	0.203
f_3^s	$\frac{4}{9\pi^2}$	0.045
f_4^s	0	0
f_5^s	$\frac{4}{25\pi^2}$	0.016
f_6^s	$\frac{2}{9\pi^2}$	0.023
f_7^s	$\frac{4}{49\pi^2}$	0.008
f_8^s	0	0
f_9^s	$\frac{4}{81\pi^2}$	0.005

Table 5.3: Values of the first 10 symmetric coefficients.

The triangular load along the circumference of the shell can be described as:

$$f(\theta) = \sum_{n=0}^{N} f_n^s \cdot \cos(n\theta) \tag{5.15}$$

In table 5.3, the first ten coefficients for the triangular load can be observed. The triangular-shaped load is built up from periodic cosine functions with different n values. As discussed, the SAFE method can obtain the properties of the shell per mode n. By applying the load coefficients to the appropriate modes, the response to each individual mode can be determined. The total response is then obtained by summing the results from each individual mode. In this manner, the response approximates the triangular load response from COMSOL. As more modes are considered, the total response increasingly approximates the real response. It will be tested to determine how many modes should be incorporated for an accurate representation.

5.4 Static analysis

Before the dynamic analysis is performed, it is important to verify how the system handles static loading. Ensuring the system can accurately find results to static load cases, before proceeding to the challenging dynamic analysis. Additionally, the static analysis ensures that boundary conditions are correctly handled.

The response of the system has a time dependence in the form of $e^{i\omega t}$. When ω is zero, this time function equals 1, indicating that the force does not change over time. By setting the forcing frequency to 0, the system simplifies to a static analysis. The equation for this static analysis becomes:

$$\mathbf{K}_n \cdot \mathbf{u}_n = F_n \tag{5.16}$$

5.4.1 Static Response of Conical Shell to Uniform Loading

To obtain the response to the uniform load, it was described that only $n = 0$ modes are active. Therefore the solution is obtained by solving the next equation for $\mathbf{u}_0$.

$$\mathbf{K}_0 \cdot \mathbf{u}_0 = \mathbf{F}_0$$

In this equation the $\mathbf{K}_n$ and $\mathbf{F}_n$ are calculated for $n = 0$ and $\mathbf{u}_0$ is obtained, resulting in:

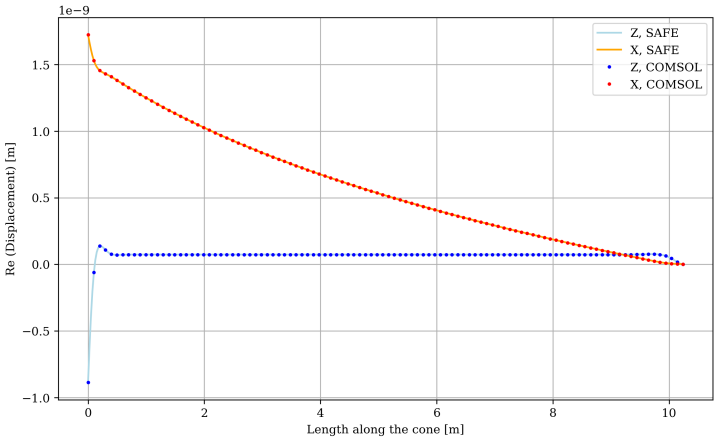

Figure 5.7: Static Response of Conical Shell to Uniform Loading

In Figure 5.7, the results of the static loading analysis are presented. The conical shell was defined with free-clamped boundary conditions, and as shown in the figure, there are no displacements at the clamped edge. The fact that the static load responses from both the COMSOL model and the SAFE method are indistinguishable confirms that the SAFE method accurately handles uniform static loads.

5.4.2 Static Response of Conical Shell to Triangular Loading

One more static analysis is performed in which the conical shell is subjected to the triangular-shaped load. This test evaluates if the SAFE method can handle non-uniform loads. By decomposing the triangular-shaped load in cosines and sines, as explained above, the total response can be calculated by summing the individual responses for each mode n.

The displacements are found by solving equation 5.16 for each n and summing them.

In the mathematical formula this will be:

$$\mathbf{u}_{total} = \sum_{n=0}^{N} \mathbf{u}_n \tag{5.17}$$

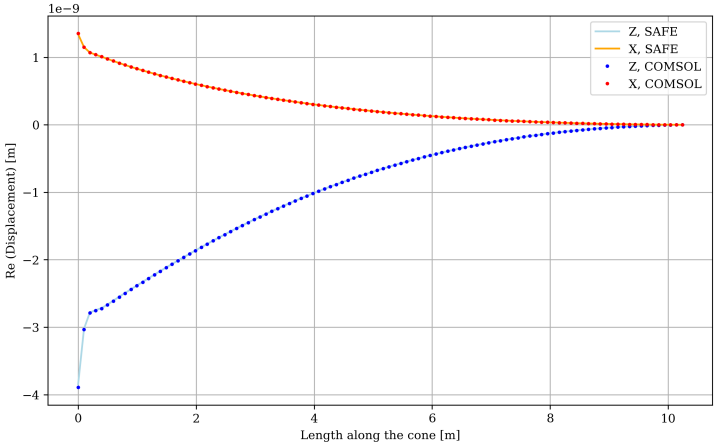

Figure 5.8: Static Response of Conical Shell to Triangular Loading

In Figure 5.8, the response to the triangular load case is shown. By observing the result, it can be concluded that the approach of decomposing the load in a series of cosines and sines and finding the response to these individual functions is a valid approach.

5.5 Harmonic Response Analysis

Now that the accuracy of the SAFE method in handling static loads has been demonstrated, the analysis proceeds with analysing the system under harmonic loading.

The forced vibration analysis will be carried out in the frequency domain, which is suitable for harmonic loading where the external forcing is frequency dependent. This simplifies the calculation of the response, which is given below by the following equation.

$$\big(-\omega^2 \mathbf{M}_n + (1 + 2\mathrm{i}\,\mathrm{sgn}(\omega)\,\xi)\,\mathbf{K}_n \big)\mathbf{u}_n = \mathbf{F}_n \tag{5.18}$$

ω is the forcing frequency of the external forcing, $\mathbf{M}_n$ and $\mathbf{K}_n$ are the mass and stiffness matrices for mode n. $\mathbf{u}_n$ is the displacement vector, ξ represents the damping ratio and $\mathbf{F}_n$ is the force vector.

Due to the application of damping in the forced vibration analysis, the response will have both real and imaginary parts. To compare the results from the SAFE method with those obtained from the COMSOL model, both the real and imaginary parts of the response will be plotted.

Similar to the static analysis, harmonic response analysis will examine both uniform-shaped and triangular-shaped loads. These analyses are conducted over a frequency range from 1 Hz to 300 Hz. Since the first few eigenmodes for both axisymmetric and non-axisymmetric cases fall within this frequency range, this frequency range will be the focus of the analysis.

5.5.1 Harmonic Response of Conical Shell to Uniform Loading

Figure 5.9 illustrates the comparison between the results obtained from the SAFE method and the COMSOL model. This figure presents a contour plot where the horizontal axis represents the coordinate along the shell, and the vertical axis represents the forcing frequency in rad/s. The plot shows the percentage difference in absolute displacements between the two methods.

This choice was made because, particularly when the forcing frequency is near the natural frequencies, either the real part or the imaginary part of the response can show significant differences between the two methods due to the unstable nature of the response near these frequencies. For instance, if the real part of the response is 100 times larger than the imaginary part, a large difference in the imaginary part alone may not affect the overall response. Thus, focusing on the absolute displacement ensures that small differences in one part do not overshadow the results in the plot.

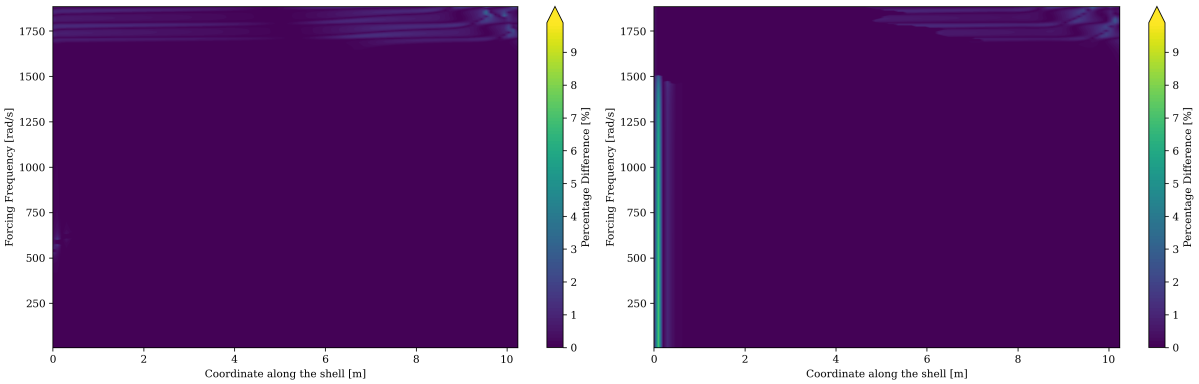

(a) Horizontal Displacements

(b) Vertical Displacements

Figure 5.9: Percentage Difference of Uniform Load Response between COMSOL and SAFE method Across Frequency and Shell Coordinate

In Figure 5.9, it can be observed that the difference is very small across all the forcing frequencies. This indicates that the SAFE method is accurately capturing the response. However, In Figure 5.9b, a vertical line can be observed where some difference is observed. This difference is attributed to the uniform meshing applied across the entire shell, which did not include finer discretisation near the location where the load is applied. This results in large displacements over a small area, making the model more prone to numerical differences between the SAFE method and the COMSOL model.

A few distinct forcing frequencies are shown in the next part, the first response presented is at 20 Hz, which is far below the first natural frequency of 244.21 Hz.

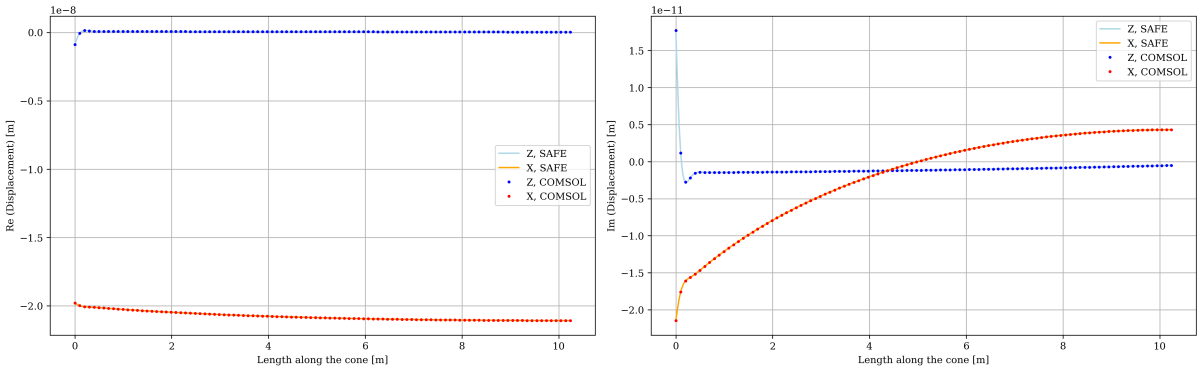

(a) Real Part (b) Imaginary Part

Figure 5.10: Displacement Comparison of Conical Shell for Uniform Loading at $f = 20$ Hz (125.66 rad/s)

Firstly, In the figure above can be seen that the displacement for every point along the cone is similar in both the longitudinal and radial direction in the real domain. The values in the imaginary part of the displacement are orders of magnitude smaller so these displacements are negligible compared to the real part of the response. Therefore, the real part of the displacements shows that the whole cone is dominated by rigid body motion when it is forced at a frequency that lies far below the first natural frequency.

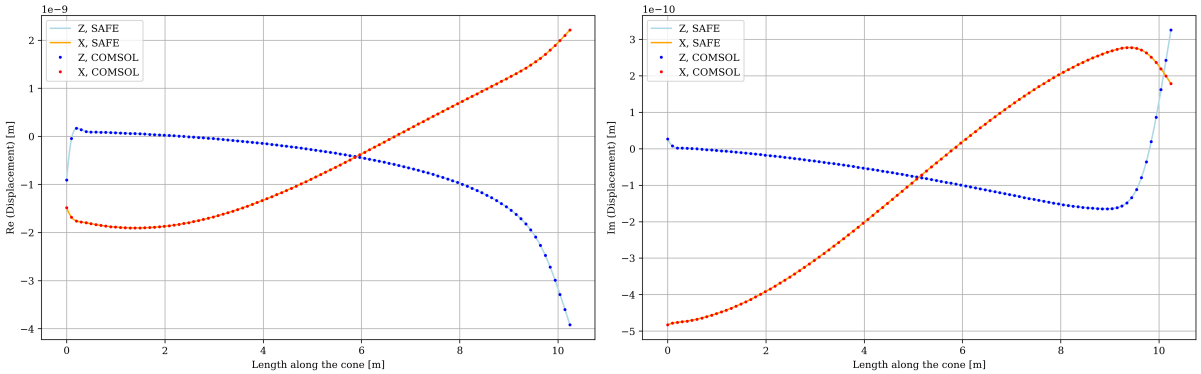

(a) Real Part (b) Imaginary Part

Figure 5.11: Displacement Comparison of Conical Shell for Uniform Loading at $f = 260$ Hz (1633.63 rad/s)

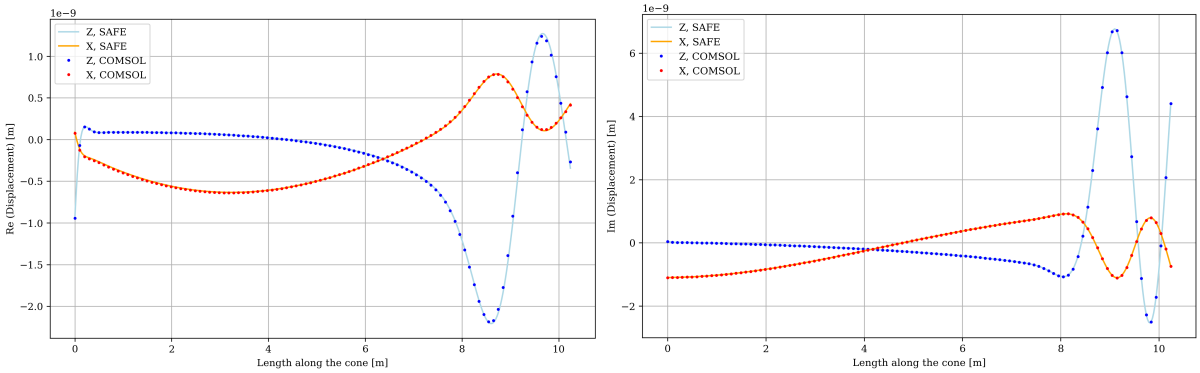

(a) Real Part

(b) Imaginary Part

Figure 5.12: Displacement Comparison of Conical Shell for Uniform Loading at $f = 297$ Hz (1866.11 rad/s)

In these figures can be seen that for the frequency of 260 Hz, the displacements from the SAFE method and the COMSOL method are for both the real and the imaginary part of the displacements again virtually indistinguishable. The real part of the displacement is again orders of magnitude larger than the imaginary part, so this is the main displacement.

In the figure of 297 Hz, this frequency excites several $n = 0$ modes. The response that is predicted by the SAFE method is very close to the response from COMSOL model.

Overall, it can be concluded that the SAFE method accurately captures the dynamic response to uniform loading across a broad frequency range.

5.5.2 Harmonic Response of Conical Shell to Triangular Loading

As described, the triangular load varies along the circumference of the shell. To determine the response to this type of load, it is first decomposed using the Fourier series. Since the Fourier series is theoretically infinite, we truncate the series after a certain number of modes. The figures illustrate the results for four different truncation points, with each case representing an increment of five additional modes. These truncated force representations are applied to the conical shell, and the results are presented in these four steps of increasing mode count. Each figure consists of four subfigures. The first two subfigures show the triangular load decomposed into the specified number of modes for that step and the difference between the analytical formulation and the triangular load. The last two subfigures display the difference plots over the frequency range and place along the shell.

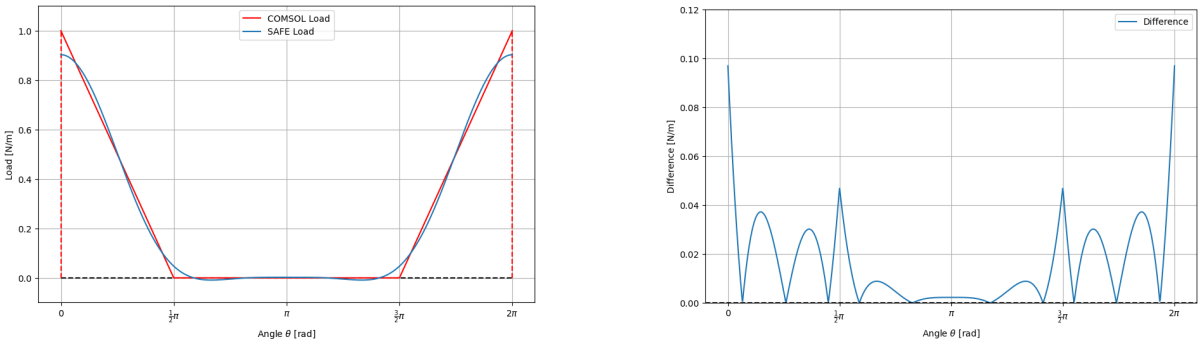

(a) Triangular Load (5 Modes)

(b) Percentage Difference Load (5 Modes)

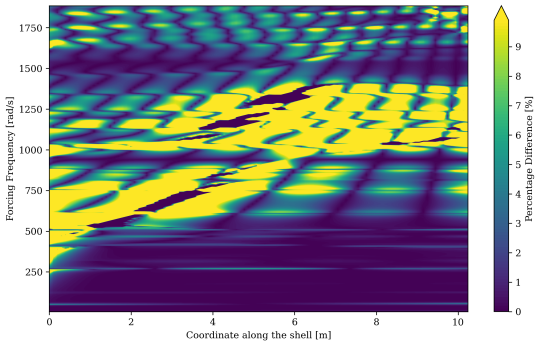

(c) Horizontal Displacements

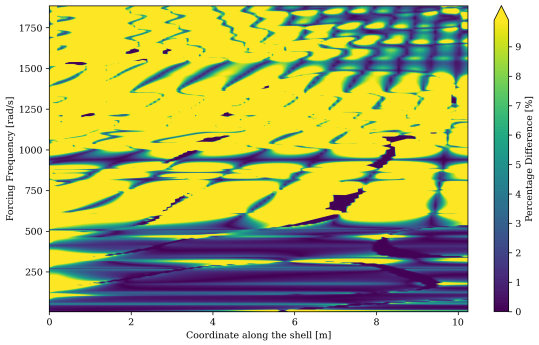

(d) Vertical Displacements

Figure 5.13: Triangular-Shaped Load Results for 5 Modes

In figure 5.13 can be observed that when only the first 5 modes are excited that the difference between the solutions from the SAFE method is significant. This indicates that more modes need to be excited to truly get the real response to the triangular loading.

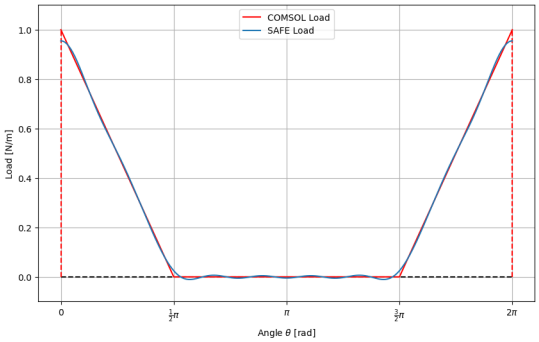

(a) Triangular Load (10 Modes)

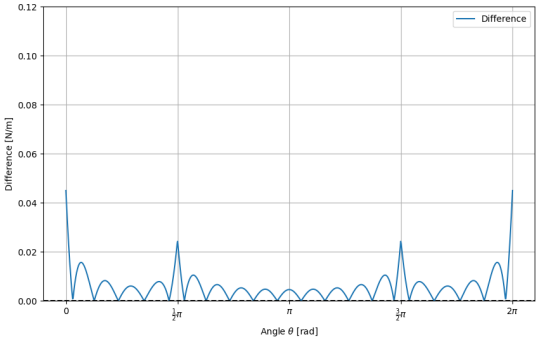

(b) Percentage Difference Load (10 Modes)

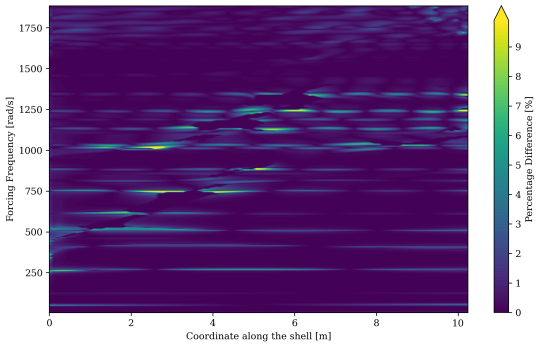

(c) Horizontal Displacements

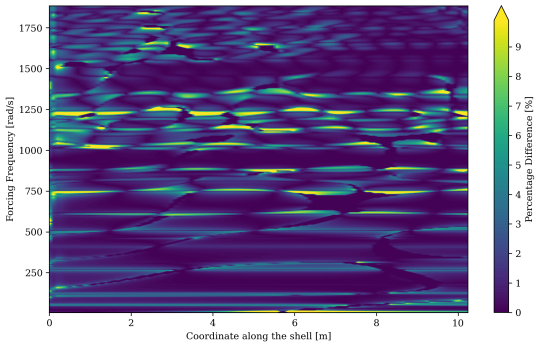

(d) Vertical Displacements

Figure 5.14: Triangular-Shaped Load Results for 10 Modes

In figure 5.14 can be observed that the result is a lot better than in the previous step. Still now can be observed that there are still some regions in the plot that show difference between the solutions.

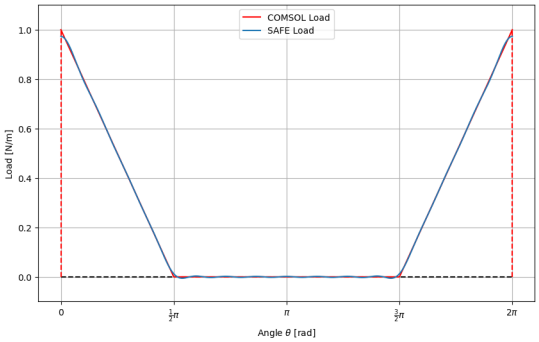

(a) Triangular Load (15 Modes)

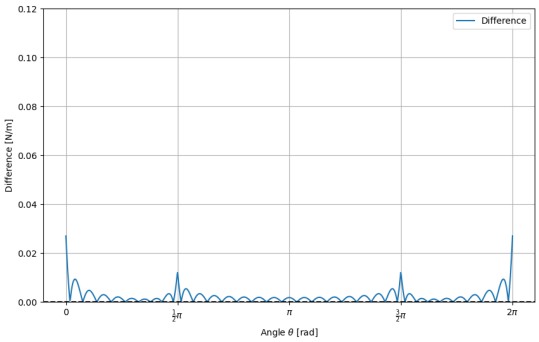

(b) Percentage Difference Load (15 Modes)

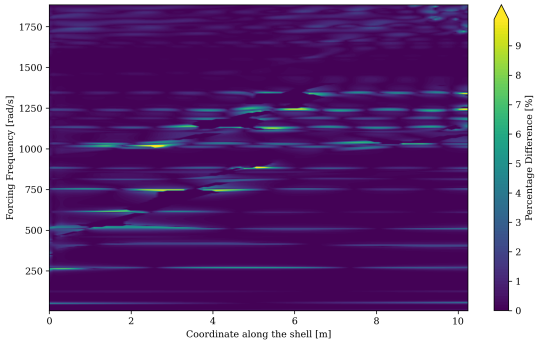

(c) Horizontal Displacements

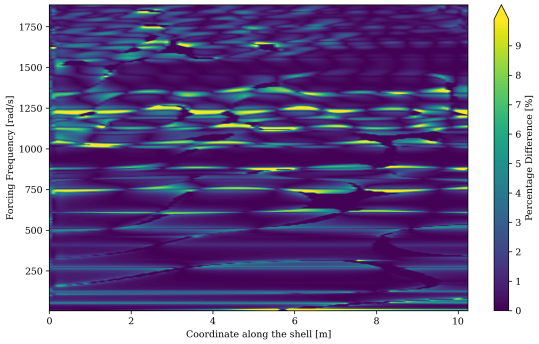

(d) Vertical Displacements

Figure 5.15: Triangular-Shaped Load Results for 15 Modes

In figure 5.15, the first 15 modes are excited and minimal change is observed compared to 10 modes. Only small improvements are observed between figure 5.15c and 5.14c.

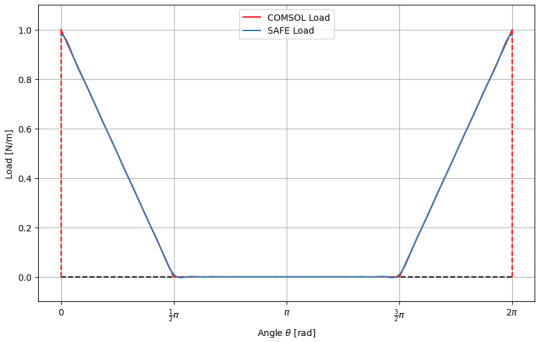

(a) Triangular Load (20 Modes)

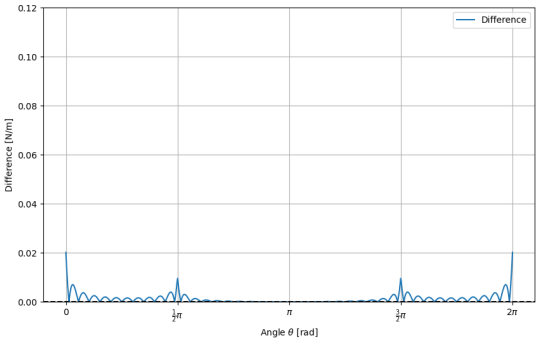

(b) Percentage Difference Load (20 Modes)

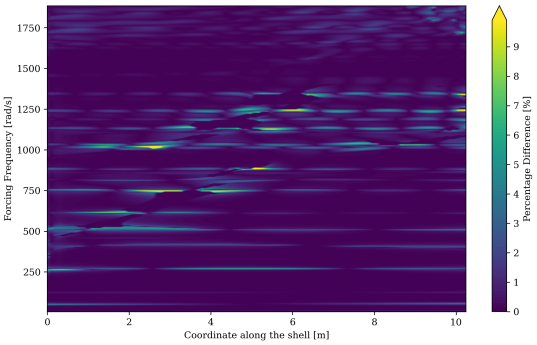

(c) Horizontal Displacements

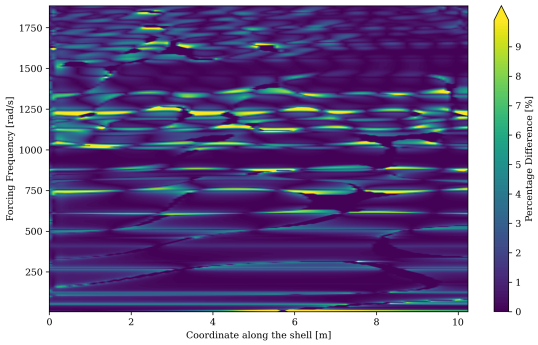

(d) Vertical Displacements

Figure 5.16: Triangular-Shaped Load Results for 20 Modes

When the first twenty modes are excited, no difference is observed compared to the first fifteen modes. The coefficients simulating the triangular response become so small that they have no impact on the response. Additionally, the natural frequencies of these high circumferential modes fall outside the range of forced frequencies in this analysis, making their response negligible.

Despite the overall accuracy, there are frequencies where the differences between the two solutions is significant, shown as yellow regions in the figures. This occurs when the forcing frequency is very close to a natural frequency of the cone. At these natural frequencies, the response can be significantly larger than at other frequencies. Since the natural frequencies of the cone calculated by SAFE are very close, but not exactly the same as those calculated by COMSOL, these small differences can result in significant difference in response when the forcing frequency is near a natural frequency. This phenomenon is illustrated in the following example of a single-degree-of-freedom system.

SDOF system

Near the eigenfrequencies, the magnitude of the response between the SAFE system and COMSOL model can be slightly different. This phenomenon will be explained within the framework of a single-degree-of-freedom (SDOF) system.

The equation of motion for a SDOF system is given by:

$$m\ddot{x}(t) + c\dot{x}(t) + kx(t) = F(t) \tag{5.19}$$

where m is the mass, c is the damping coefficient, k is the stiffness $x(t)$ is the displacement as a function of time and $F(t)$ is the external force.

When subjected to a harmonic excitation, $F(t) = F_0 \cos(\omega t)$, the steady state response is given by:

$$x(t) = |H(\omega)| F_0 \cos(\omega t + \phi) \tag{5.20}$$

Where $|H(\omega)|$ is the magnitude of the response:

$$|H(\omega) = \frac{1}{(k - m\omega^2)^2 + (c\omega)^2} \tag{5.21}$$

The values for these parameters are taken as:

$$\begin{aligned} k &= 1000\,\text{N/m} \\ m &= 10\,\text{kg} \\ c &= 0.1\,\text{Ns/m} \\ \Delta m &= 0.1\,\text{kg} \end{aligned}$$

The damping ratio is calculated by:

$$\zeta = \frac{c}{2\sqrt{km}} = \frac{0.1}{200} = 0.0005 \tag{5.22}$$

The system is lightly damped, because $\zeta = 0.0005 << 1$

To illustrate how the response varies near the natural frequency, the magnitude of the frequency response will be examined for both masses m and $m + \Delta m$. This results in the following figure:

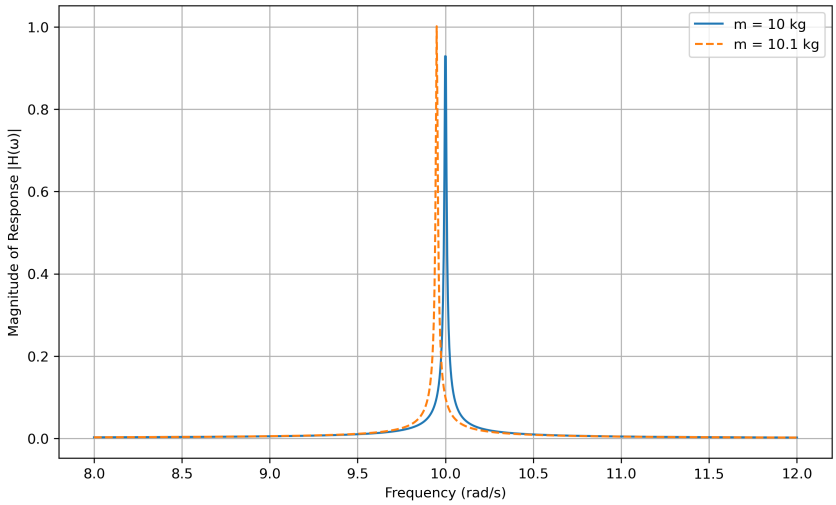

Figure 5.17: Magnitude response of SDOF system

The figure illustrates that the magnitude of the response of a lightly damped single degree of freedom (SDOF) system is highly sensitive near its natural frequency. A 1 % difference in mass shifts the response function slightly to the left. At a exactly the frequency of 10 rad/s, the magnitude of the response of the system with mass $m + \Delta m$ is significantly less than the one with mass m. Specifically, the magnitude of the response for $m + \Delta m$ is only 11% of that for m. In conclusion, even though the systems are very similar, the response can vary greatly with slight differences in the system. Here, it is shown for a difference in mass, but the same principle holds for differences in stiffness or damping.

Because the SAFE system and COMSOl model are calculated differently, this phenomenon can also occur between these two methods. Therefore, the response of the systems near natural frequencies must be examined cautiously, and differences between the methods should not automatically invalidate either one.

Now the response of a few frequencies are shown.

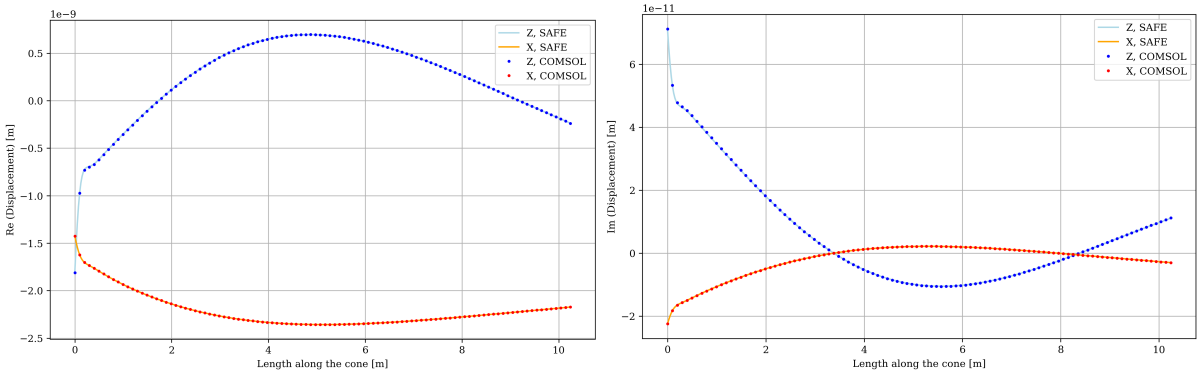

(a) Real Part

(b) Imaginary Part

Figure 5.18: Displacement Comparison of Conical Shell for Uniform Loading at $f = 32$ Hz (201.06 rad/s)

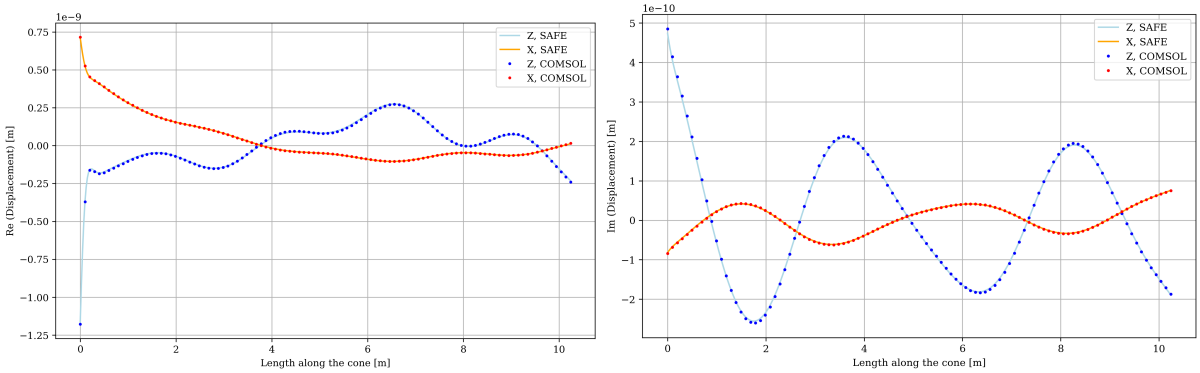

(a) Real Part (b) Imaginary Part

Figure 5.19: Displacement Comparison of Conical Shell for Uniform Loading at $f = 176$ Hz (1105.84 rad/s)

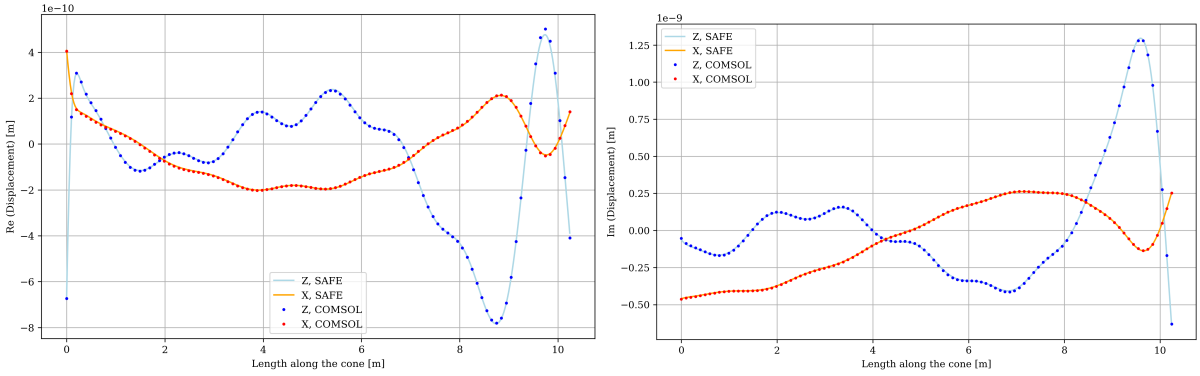

(a) Real Part (b) Imaginary Part

Figure 5.20: Displacement Comparison of Conical Shell for Uniform Loading at $f = 285$ Hz (1790.71 rad/s)

As observed in the section, the SAFE method can obtain many dynamic characteristics of the conical shell. It is shown that the SAFE method can accurately capture the natural frequencies of the system for both axisymmetric and non-axisymmetric modes. Additionally, the SAFE method is also capable of obtaining the static response of the system to a static load and handling boundary conditions as needed. Both the response to the uniform loading and triangular shaped load gave accurate results. The conical shell was then subjected to a dynamic load. The dynamic response to the uniform loading, across all forcing frequencies, showed little difference, indicating that the method is functioning correctly. Also the dynamic response to the triangular-shaped loading gave accurate results for the most part. Therefore, it can be stated that the developed semi-analytical numerical framework for conical shells has succeeded.

In the next chapter, the conical shell will be coupled to a cylindrical shell and the same analyses as for the conical shell will be conducted and reported on.

Chapter 6

Results and Analysis of the Coupled Conical-Cylindrical Shell

In practice, piles with large dimensions can be considered as conical shells coupled with cylindrical shells. Therefore, we aim to have a numerical framework that is capable of coupling conical shell elements to cylindrical shell elements. Currently, the numerical framework depends on the conical shell angle α. By setting this angle to zero, cylindrical elements can be obtained.

During the development of the numerical framework it was ensured that when the angle α of the conical shell is set to zero, the solution of the cylindrical shell is obtained. For constructing a conical shell element with this framework, the axis on which the displacements are calculated depends on the angle α. These axes are aligned with the inclination of the shell elements. Axial displacements are always in the same direction as the inclination of the shell and the radial displacement always perpendicular to this inclination.

When the element stiffness and mass matrices are constructed, they are calculated in the local axes system. To perform any analysis, we therefore have to rotate the stiffness matrices per element to a global coordinate system. In these analyses, the global axes were taken along the cylindrical shell (horizontal and vertical). The stiffness matrices of the conical elements are rotated before assembling into the global stiffness matrix. After this procedure, the same analyses are performed, similar to those on the conical shells. This will serve as a validation that this method of combining different elements is a valid approach of coupling systems.

First, the natural frequencies for axisymmetric ($n = 0$) and non-axisymmetric ($n = 1$) will be compared with those obtained from COMSOL. Following this, the mode shapes that arise will be compared. And finally, the forced vibration study will be conducted on the coupled conical-cylindrical system, same as performed on the conical shell.

The properties of the coupled conical-cylindrical are listed in table 6.1.

Geometrical Properties Cone	**Value**	**Unit**
Radius left	0.8	m
Radius right	3.0	m
Length	5.0	m
Geometrical Properties Cylinder		
Radius	3.0	m
Length	5.0	m
Material Properties	**Value**	**Unit**
Density (ρ)	7850	kg/m^3
Poisson's ratio (ν)	0.3	-
Thickness (h)	0.0159	m
Young's modulus (E)	210	GPa

Table 6.1: Geometrical and Material Properties of the Coupled Conical-Cylindrical Shell

6.1 Free Vibration Analysis

After obtaining the global stiffness and mass matrix, the free vibration analysis can be performed. By setting the force to zero and substituting the assumed solution for the displacements we get to the same eigenvalue problem as previously seen:

$$(-\omega_{nj}^2 \mathbf{M}_n + \mathbf{K}_n)\mathbf{u}_{nj} = \mathbf{0} \tag{6.1}$$

The boundary conditions that will be considered in the free vibration analysis are free-free. Again, the axisymmetric case ($n = 0$) and the non-axisymmetric case ($n = 1$) will be investigated.

Axisymmteric Modes $n = 0$

The result for the natural frequencies of the coupled conical-cylindrical shell for the axisymmetric motion is presented in the following figure:

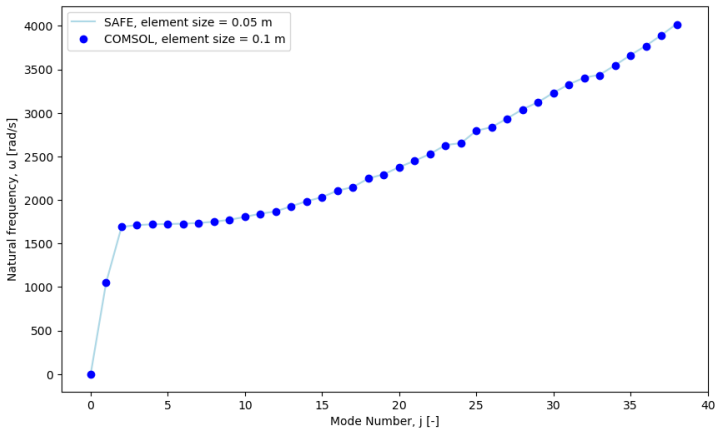

Figure 6.1: Comparison of Natural Frequencies Between Comsol and SAFE Method for $n = 0$ modes

In the analysis of natural frequencies for the conical shell, it was observed that the element size from the mesh in SAFE provided accurate results for an element size of 0.05 m. Therefore this was used again in this analysis on the coupled conical-cylindrical shell. Because the geometry of the coupled conical-cylindrical shell is more complex than just a conical shell, the eigenfrequency analysis was performed more extensively. In this analysis, the first 2000 natural frequencies were calculated in COMSOL, compared to the 1000 natural frequencies calculated in the same analysis on conical shells. In 6.1, now the first 40 natural frequencies are shown for the axisymmetric motion. As can be seen in table 6.2, the analysis in COMSOL took almost seven hours to complete. In comparison with the SAFE method that still completes the analysis in 0.2 seconds. Showing the potential of the SAFE method once again.

In the table below can be seen

	SAFE	**COMSOL**
Elements	200	20160
DoF	804	487296
Total Time	0.2s	6h54m
Time per mode	0.0002s	12.42s

Table 6.2: Comparison of SAFE and COMSOL simulations.

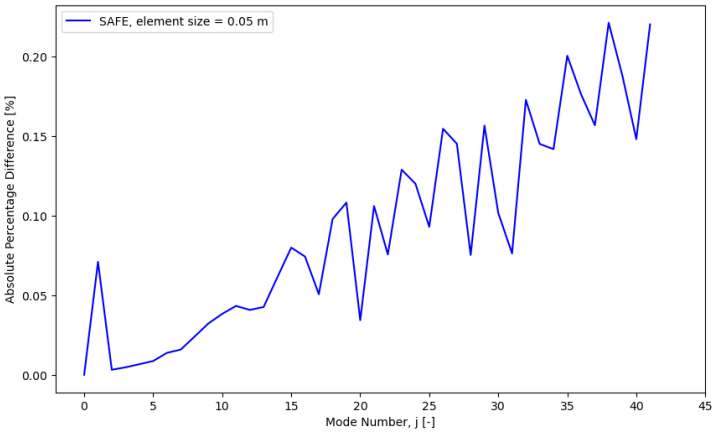

Figure 6.2: Difference between SAFE Method and COMSOL for $n = 0$ modes

In figure 6.2 can clearly be seen that the natural frequencies calculated by the SAFE method are close to the natural frequencies calculated by COMSOL. Still for the 40th eigenfrequency, there is only a 0.2% difference between COMSOL and SAFE.

Non-Axisymmetric Modes $n = 1$

Same procedure is done for non-axisymmetric modes with $n = 1$:

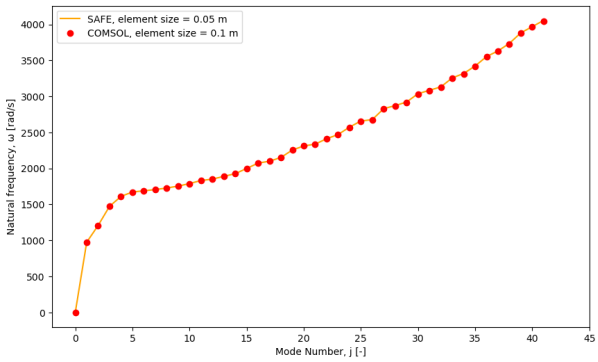

Figure 6.3: Comparison of Natural Frequencies Between Comsol and SAFE Method for $n = 1$ modes

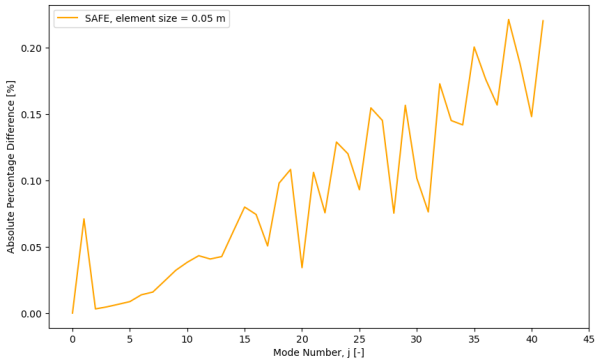

Figure 6.4: Difference between SAFE Method and COMSOL for $n = 1$ modes

It can be concluded that the SAFE method gives very accurate results for the natural frequencies of the coupled conical-cylindrical shell system for both axisymmetric modes ($n = 0$) and the non-axisymmetric modes ($n = 1$)

6.2 Comparison of Eigenmodes

For further validation, the eigenmodes that are linked to the found natural frequencies are inspected. In the same way as for the conical shells, after obtaining the natural frequencies, the corresponding eigenmodes are calculated. The displacements are again normalised with the horizontal displacement of the left boundary of the shell.

Eigenmodes $n = 0$

The first five eigenmodes for $n = 0$ are presented in figure 6.5:

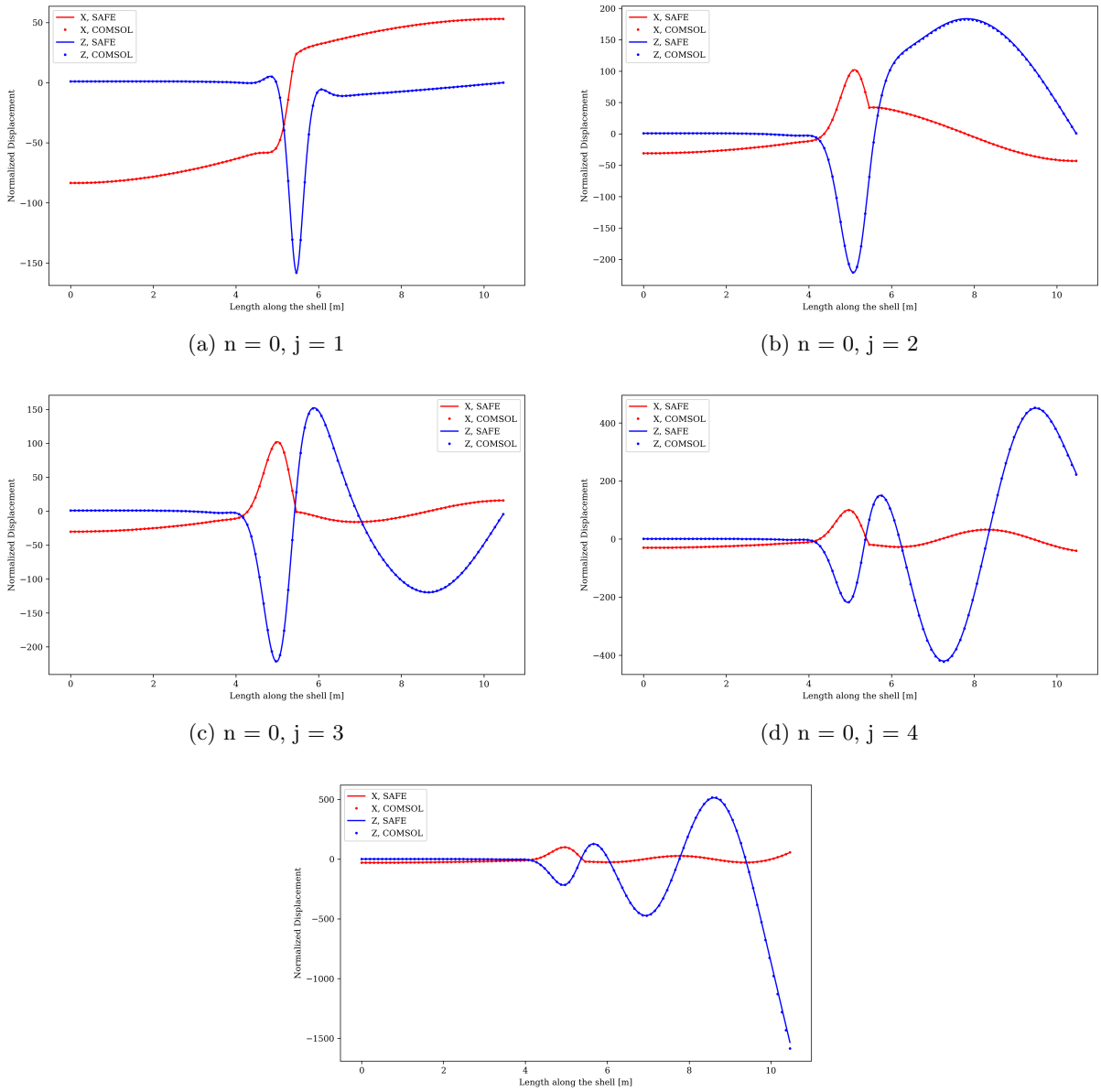

(a) n = 0, j = 1

(b) n = 0, j = 2

(c) n = 0, j = 3

(d) n = 0, j = 4

(e) n = 0, j = 5

Figure 6.5: Mode shaped Coupled Conical-Cylindrical shell, n = 0

Eigenmodes $n = 1$

Similarly, the first five eigenmodes for $n = 1$ are shown in figure 6.6

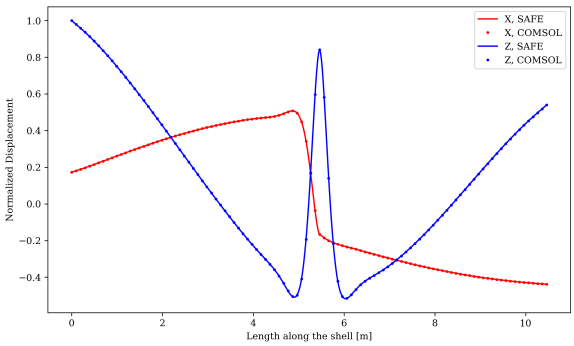

(a) n = 1, j = 1

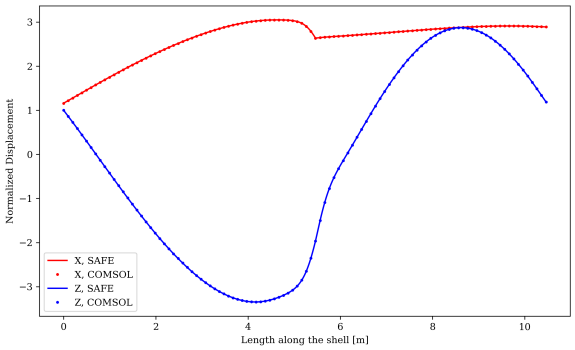

(b) n = 1, j = 2

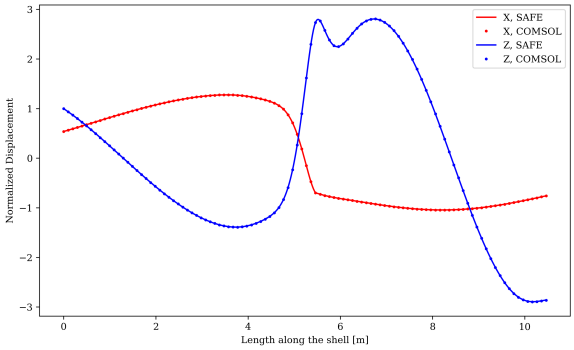

(c) n = 1, j = 3

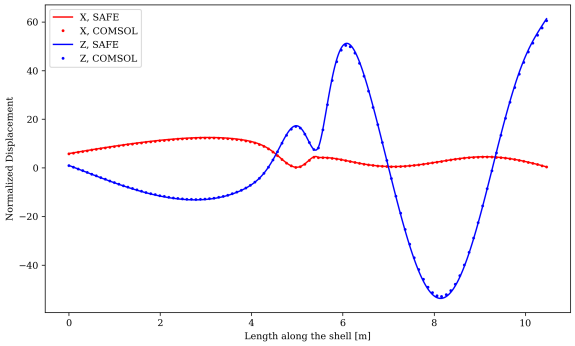

(d) n = 1, j = 4

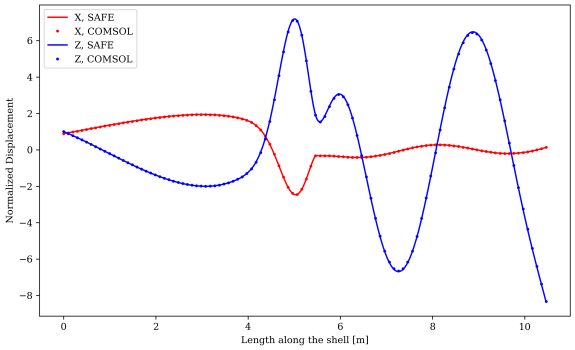

(e) n = 1, j = 5

Figure 6.6: Mode shaped Coupled Conical-Cylindrical shell, n = 1

The comparison shows excellent agreement for all the eigenmodes presented. This consistency in natural frequencies and the corresponding mode shapes confirms that the method of coupling conical elements with cylindrical elements to determine the vibrational characteristics of the conical-cylindrical shell is both valid and reliable. These results motivate continuing with the validation of the method.

6.3 Static Analysis

Before continuing to the dynamic analysis, first the coupled conical-cylindrical shell is subjected to a static analysis for both loading. The boundary conditions for the static loading case are again chosen to be free-clamped.

6.3.1 Static Response of Coupled Conical-Cylindrical Shell to Uniform Loading

The static response of the coupled conical-cylindrical shell under uniform loading is illustrated in Figure 6.7

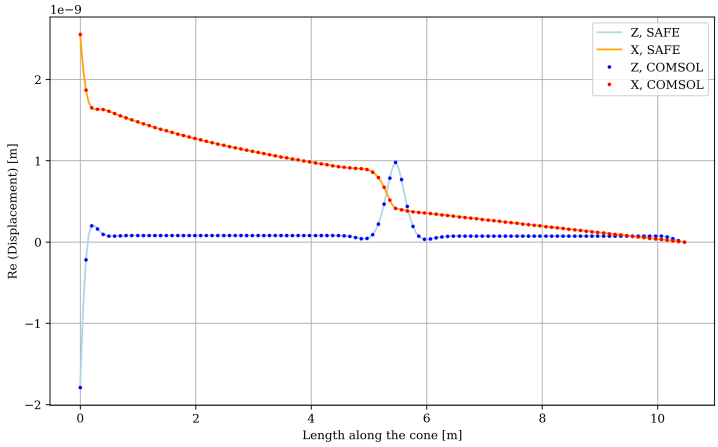

Figure 6.7: Static Response of Coupled Conical-Cylindrical Shell to Uniform Loading

6.3.2 Static Response of Coupled Conical-Cylindrical Shell to Triangular Loading

Figure 6.8, illustrates the static response of the shell when subjected to a triangular-shaped load distribution.

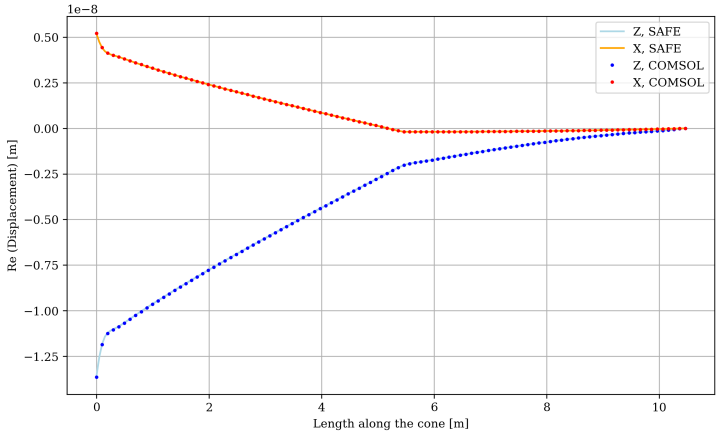

Figure 6.8: Static Response of Coupled Conical-Cylindrical Shell to Triangular Loading

Both responses being accurate indicates that the free-clamped boundary conditions have been correctly implemented in the SAFE method, and that the loading has been applied appropriately.

6.4 Harmonic Response Analysis

In this section the harmonic response is shown for the coupled conical-cylindrical shell to two types of loading. First, the results to the uniformly distributed load are presented. Following this, the results to the triangular-shaped loading are shown. The range of frequencies that is investigated is 1 Hz to 300 Hz with incremental steps of 1 Hz.

6.4.1 Harmonic Response of Coupled Conical-Cylindrical Shell to Uniform Loading

In Figure 6.9, the response along the shell, for each forcing frequency in the range from 1 Hz to 300 Hz, can be observed.

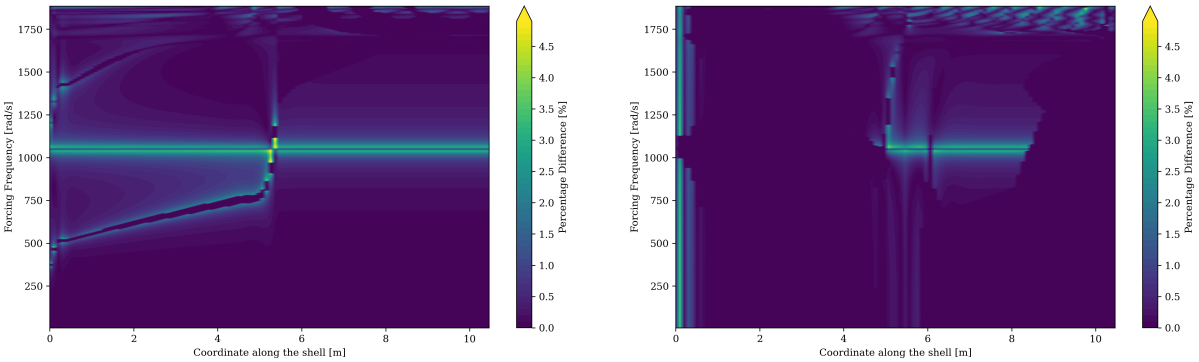

(a) Horizontal Displacements

(b) Vertical Displacements

Figure 6.9: Percentage Difference of Uniform Load Response between COMSOL and SAFE method Across Frequency and Shell Coordinate

Notably, is the horizontal line where some difference is observed. This line occurs at the first natural frequency of the $n = 0$ modes. As explained in the previous chapter, this phenomena could happen if the forcing frequency is in proximity to a natural frequency of the system.

The vertical line that can be observed in 6.9b can be attributed to the mesh being evenly distributed. Since the force is applied at the edge, it can cause localised deformations. This localisation results in small differences between the methods due to the high sensitivity of the mesh in regions with significant displacement. As seen, relatively large displacement in the vertical direction happens in a short area, which leads to the difference observed.

Overall, the results illustrate that the SAFE method and the COMSOL model are in agreement.

For a few different frequencies the results are shown again in the following figures:

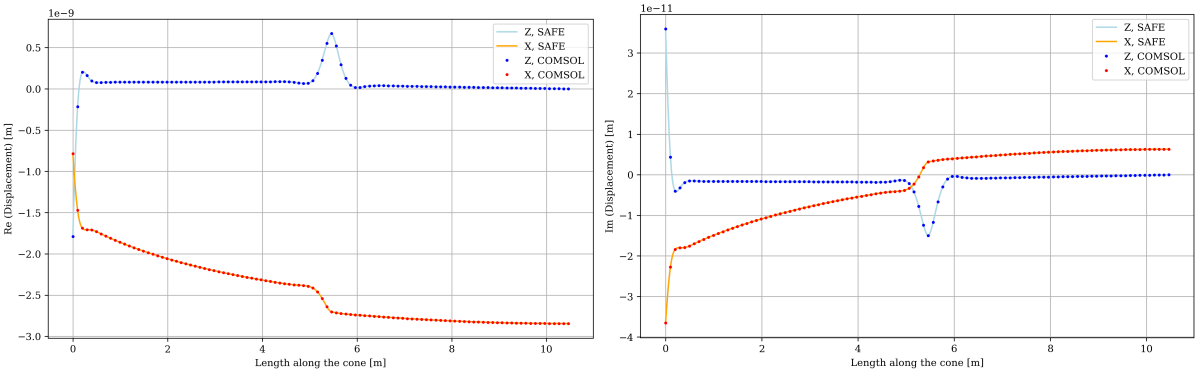

(a) Real Part

(b) Imaginary Part

Figure 6.10: Harmonic Response to Uniform Loading at $f = 50$ Hz ($\omega = 314.16$ rad/s)

In Figure 6.10, can be observed that at the left, a relatively large response is present. This is due to the loading being applied at that edge. This frequency is far below the first natural frequency of the coupled shell, therefore the displacements is smooth. The noticeable part is at the connection between the conical and the cylindrical part. The SAFE method is capable of obtaining the response accurately.

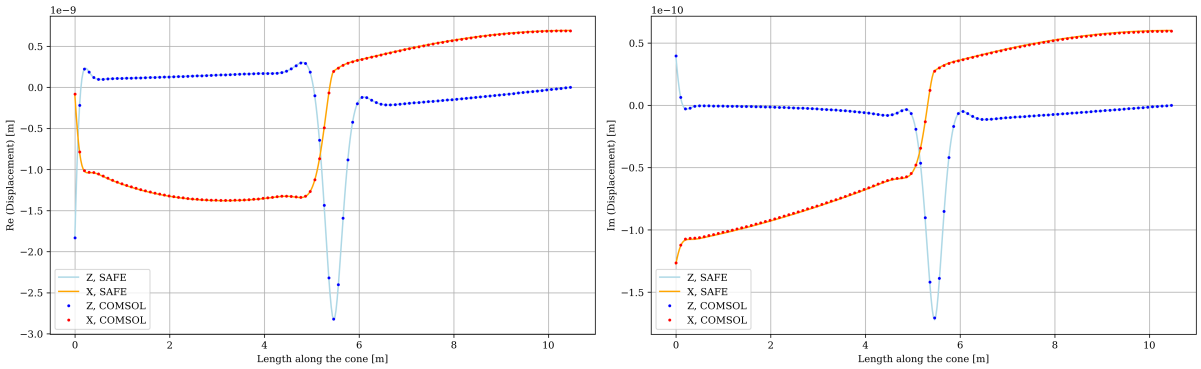

(a) Real Part (b) Imaginary Part

Figure 6.11: Harmonic Response to Uniform Loading at $f = 190$ Hz ($\omega = 1197.2$ rad/s)

Figure 6.11, shows the response to a frequency that is located between the first and natural frequency. The response is similar in shape as the first eigenmode of the system.

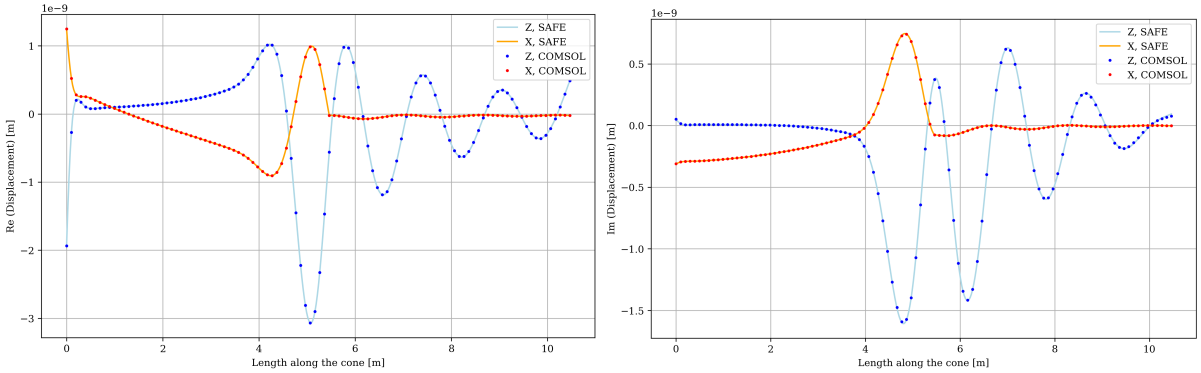

(a) Real Part (b) Imaginary Part

Figure 6.12: Harmonic Response to Uniform Loading at $f = 280$ Hz ($\omega = 1760.0$ rad/s)

Figure 6.12, shows the response to a frequency that is above several natural frequencies. As can be seen, the response is accurately captured.

6.4.2 Harmonic Response of Coupled Conical-Cylindrical Shell to Triangular Loading

In this section the triangular-shaped load is applied with incorporating a different amount of modes. The same procedure as for the conical shell is considered, the results to four steps of loading are presented.

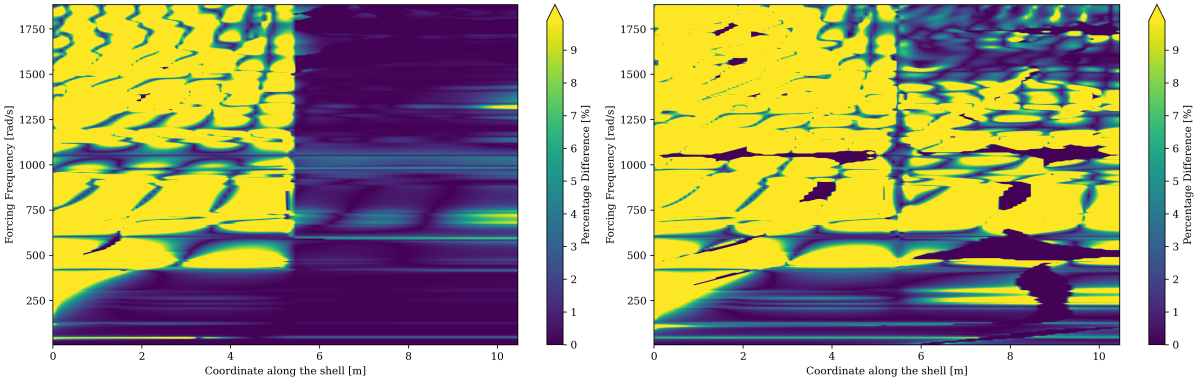

(a) Horizontal Displacements (b) Vertical Displacements

Figure 6.13: Percentage Difference of Triangular Load Response between COMSOL and SAFE method Across Frequency and Shell Coordinate, 5 modes

In Figure 6.13, it can be observed that there is a noticeable difference between the results obtained using the SAFE method and those from the COMSOL model across the entire frequency range. This difference appears because an insufficient number of modes was considered, leading to inaccurate responses throughout the frequency range.

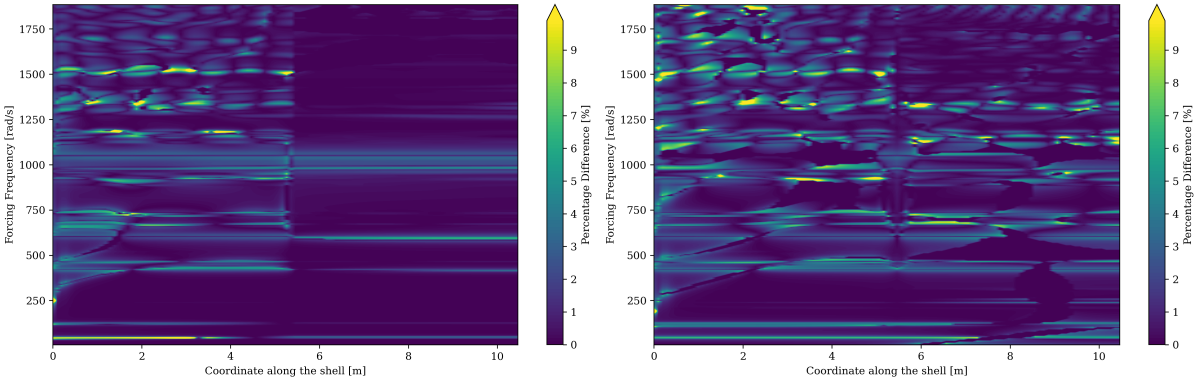

(a) Horizontal Displacements (b) Vertical Displacements

Figure 6.14: Percentage Difference of Triangular Load Response between COMSOL and SAFE method Across Frequency and Shell Coordinate, 10 modes

In Figure 6.14 is shown that ten considering ten modes instead of five, gives better results across the whole frequency range. There is still some difference shown in the plots, so the analysis will continue to incorporate the first fifteen modes. These results will be shown in the next figure.

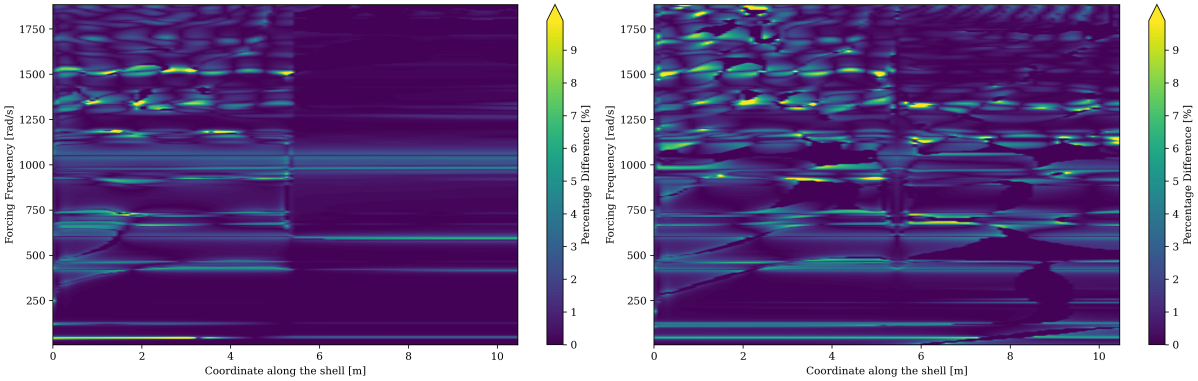

(a) Horizontal Displacements (b) Vertical Displacements

Figure 6.15: Percentage Difference of Triangular Load Response between COMSOL and SAFE method Across Frequency and Shell Coordinate, 15 modes

A minimal amount of change is observed between figures 6.14 and 6.15. Therefore, the analysis continues with the first twenty modes:

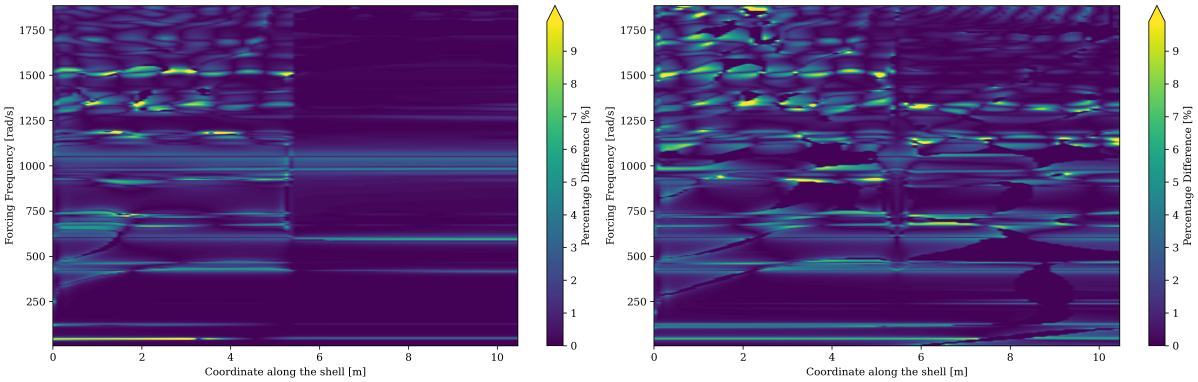

(a) Horizontal Displacements (b) Vertical Displacements

Figure 6.16: Percentage Difference of Triangular Load Response between COMSOL and SAFE method Across Frequency and Shell Coordinate, 20 modes

No change is observed between the incorporation of the first fifteen modes and the first 20 modes. Overall, in Figure 6.16, for frequencies that are not located near natural frequencies, agreement is found between the two methods. Despite the overall accuracy, there are frequencies where the difference between the two solutions is significant, shown as yellow regions in the figures. This occurs when the forcing frequency is very close to a natural frequency of the cone. The same reasoning for this is explained in this analysis on the conical shells.

The kinks in the displacement graphs are due to the connection between the conical and coupled conical-cylindrical shell. For a few frequencies, the response is shown, the X axis is defined as the horizontal axis, while the Z axis is the vertical axis:

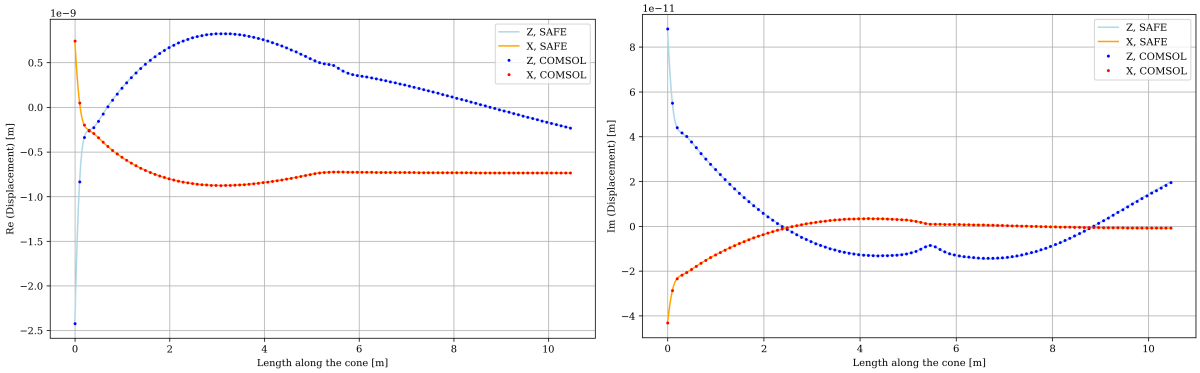

(a) Real Part (b) Imaginary Part

Figure 6.17: Harmonic Response to Triangular Loading at $f = 50$ Hz (314.16 rad/s)

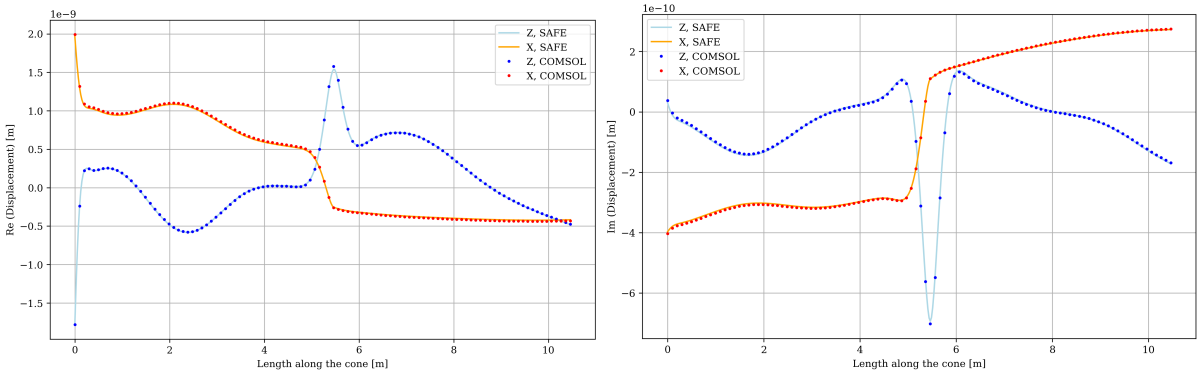

(a) Real Part (b) Imaginary Part

Figure 6.18: Harmonic Response to Triangular Loading at $f = 160$ Hz (1005.31 rad/s)

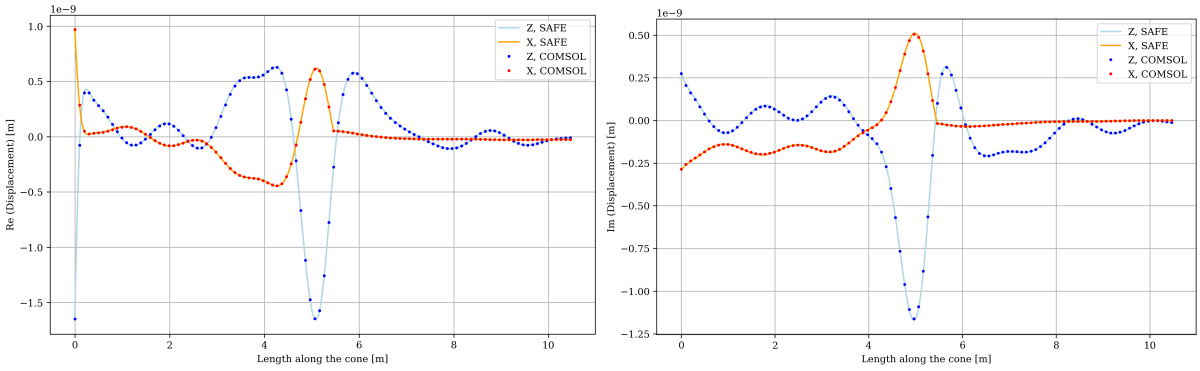

(a) Real Part (b) Imaginary Part

Figure 6.19: Harmonic Response to Triangular Loading at $f = 275$ Hz (1727.88 rad/s)

In this chapter the results for the coupled conical-cylindrical shell were presented. It can be concluded that the method for assembling the conical shell elements with cylindrical elements to construct the coupled conical-cylindrical shell is valid. The results presented show the agreement between the results obtained by the SAFE method and those obtained from COMSOL.

Chapter 7

Conclusion

This thesis set out to develop and validate a semi-analytical finite element (SAFE) model for conical shells. Starting from the general equations of motion, kinematic and constitutive equations, and boundary conditions from Leissa's "Vibration of Shells," the semi-analytical finite element model was specifically developed for a conical shell.

Objective and Methodology
The main goal was to create a numerical framework capable of accurately predicting the dynamic characteristics of conical shells, including the natural frequencies, mode shapes, and harmonic responses to loading. An important objective was to ensure that this framework is robust and versatile, allowing it to be used as easily as 1D elements and to be coupled with other elements easily. The SAFE method integrates the semi-analytical approach by discretising the axial direction using finite elements, while representing the circumferential displacements with analytical functions. Because the geometry of conical shells is circular in the circumferential direction, these displacements can be assumed to be analytical functions like sine or cosine, which have the property that after one revolution, the displacement returns to the same value. This approach aims to achieve a numerical framework that is both computational efficient and accurate.

Methodology
The semi-analytical finite element model was validated by comparing its results to those obtained from COMSOL Multiphysics, a widely used finite element software. This validation process involved comparing natural frequencies and corresponding mode shapes by solving the undamped eigenvalue problem. Additionally, the conical shell was subjected to harmonic forcing to determine its harmonic responses. To ensure a comprehensive dynamic analysis, this study covered a frequency range from 1 Hz to 300 Hz in 1 Hz increments. The harmonic response analysis was performed for two types of loading: a uniform harmonic load and a triangular-shaped harmonic load.

To enhance the comparison between the SAFE method and the COMSOL model, hysteretic damping was incorporated into the harmonic response analysis. First, the uniform harmonic load was applied to ensure that the SAFE method was able to accurately capture the response to the axisymmetric ($n = 0$) motion. Once this accuracy was confirmed, the analysis progressed to a more complex type of loading: a triangular-shaped harmonic load. This second type of loading, involved the excitation of multiple modes to approximate the response under the triangular-shaped load.

Another key objective was to ensure that the framework is robust and versatile, enabling it to be easily coupled to other elements. To show this capability, a conical shell was coupled to a cylindrical shell. The same analyses performed on the conical shell, were also performed on the coupled conical-cylindrical shell. This approach verified that the numerical framework can manage more complex geometries while maintaining computational efficiency and accuracy.

Key findings
Overall, it was observed that the eigenfrequencies obtained by the SAFE method, were very close to those found by the COMSOL model for the conical shell. This agreement provided confidence in the functioning of the SAFE model. Further validation involved inspecting the eigenmodes corresponding to these natural frequencies.

To further validate the SAFE method, the mode shapes associated with the obtained natural frequencies were compared to those from COMSOL. For consistency in the comparison, the modes are normalised by the displacement on the left side of the cone (U displacement). It was found that the

first five modes for both the axisymmetric modes ($n = 0$) and the non-axisymmetric ($n = 1$) modes are virtually indistinguishable between the SAFE method and COMSOL.

The close similarity between the natural frequencies and corresponding mode shapes from both COMSOL and the SAFE method suggests that the SAFE model accurately captures the structural behavior of the conical shell. This reinforces confidence in the reliability of the SAFE method's results.

Following the validation through natural frequencies and mode shapes, the validation was extended with a forced vibration analysis to evaluate the SAFE method under external excitation. This analysis involved determining the harmonic response to two types of harmonic loading: a uniform harmonic load and a triangular-shaped harmonic load. The system was damped using hysteretic damping, resulting in a response that includes both real and imaginary components. The harmonic response was determined over a frequency range from 1 Hz to 300 Hz in 1 Hz increments.

For the uniform harmonic load, which activates only the $n = 0$ modes, the response was found to be very accurate across almost all frequencies. A few forcing frequencies were shown in particular and the response was virtually indistinguishable between the SAFE method and the COMSOL model.

After confirming the accuracy of the response to uniform harmonic loading, the analysis proceeded with the triangular-shaped harmonic load. This load is first decomposed in periodic functions, represented as a sum of sine and cosine terms for different n values. By determining the system's response to each term and summing them, the total response to the triangular-shaped load is obtained.

The response to the triangular-shaped harmonic loading was fairly accurate when a sufficient number of modes were considered. Although some difference was observed between the SAFE method and the COMSOL model for certain frequencies, this was anticipated. To replicate the triangular-shaped load, twenty modes were considered. Each mode has its distinct natural frequencies, and in the case of the triangular loading, more of these modes are activated. Therefore, in the case of triangular loading, the system can be excited in many more natural frequencies. Forcing near natural frequencies, can result in large resonance, meaning that small perturbations in the forcing frequency can lead to considerable differences in results. Therefore, these observed differences do not undermine the validity of the SAFE method. A few forcing frequencies were shown in particular where the forcing frequency was not near any natural frequency. At these frequencies, the response was virtually indistinguishable between the SAFE method and the COMSOL model.

After validating the SAFE method for the conical shell, the analysis was extended to a coupled conical-cylindrical shell. The same set of analyses was performed, including the eigenvalue problem analysis. The comparison of natural frequencies for 40 modes revealed that the results for both $n = 0$ and $n = 1$ modes were very similar between the SAFE method and the COMSOL model. Specifically, the difference between the SAFE method and COMSOL for the 40th mode was only 0.2%. Additionally, the first five eigenmodes for both $n = 0$ and $n = 1$ were indistinguishable between the SAFE method and the COMSOL model.

The fact that also these results for the coupled conical-cylindrical are similar between SAFE and COMSOL, indicates that the coupling approach is valid. To further validate this coupling approach, the system was analysed using harmonic response analysis, similar to the procedure performed for the conical shell.

For both the uniform loading and the triangular loading on the coupled shell, similar results were obtained as for the conical shell. In particular for the uniform loading, a horizontal line can be observed where some difference is present. This line occurs near the first natural frequency of the $n = 0$ modes. As previously explained, this difference near natural frequencies is expected due to resonance effects.

In the response to the triangular-shaped loading for the coupled conical-cylindrical shell, the same resonance effects are observed as in the analysis on the conical shell for the same load. These differences can be explained using the same principles previously discussed.

Significance of Findings

The results presented in this work, show the potential of the SAFE method for the analysis of conical shells. The SAFE method has demonstrated its ability to accurately predict natural frequencies and mode shapes. Additionally, it is shown that the SAFE method can accurately obtain the response to various types of loading, including complex loads such as the triangular-shaped load. The success in static and harmonic analysis show that this method could be applied effectively in various applications, where different loading and boundary conditions are present.

The developed SAFE method offers several advantages over the traditional finite element method. By making use of the inherent geometric properties of closed shells and representing the circumferential displacements as harmonic functions, the SAFE method simplifies the analysis and significantly improves

computational efficiency. This approach allows for the calculation of natural frequencies, mode shapes, and responses to loading in much less computational time.

Additionally, the ease of use of the SAFE method significantly reduces the time required to set up the model compared to traditional finite element software. Traditional finite element software, can take extensive time for building the geometry, specifying the load and boundary conditions and performing the analyses. In contrast, the SAFE method simplifies these steps, allowing the input of geometrical and material properties to be completed in just one minute. This reduction in setup time, combined with the method's accuracy and computational efficiency, shows the substantial potential of the SAFE method once more.

Limitations and Future work

While it is shown that the SAFE method is very robust and versatile, some limitations need to be acknowledged.

First, the analyses were limited to linear behavior. Non-linear behavior, which would include large deformations, heterogeneous material along the thickness, was not modelled. This means that the SAFE method is not applicable in the case of conditions that induce severe non-linearity.

Future research could address this non-linearity. For example, by modifying the SAFE method to include varying material properties along the thickness, the SAFE method could be improved.

While this thesis demonstrated the method's capability to couple conical shells to cylindrical shells, future studies could explore the coupling between other types of elements. It would be a matter of obtaining the stiffness and mass matrix for the specific element and assembling them in the same way as was shown for the conical-cylindrical shell.

An additional direction for future research might be to apply the SAFE method to structures subjected to impact or transient loading, as opposed to only harmonic loading. This would help to extend the method's scope and evaluate its effectiveness under different loading conditions.

In conclusion, the successful development and validation of the SAFE method for conical shells, including its ability to couple with other elements, offers a computationally efficient and accurate approach for determining the dynamic characteristics of various shell structures. The method's robustness and versatility make it a valuable asset for both academic research and practical applications, providing and easy-to-use tool for engineers and researchers.

Bibliography

[1] Arthur W Leissa. *OF SHELLS NATIONAL AERONAUTICS AND SPACE ADMINISTRATION*. Tech. rep.

[2] Chih Ping Wu and Hao Yang Huang. "A semianalytical finite element method for stress and deformation analyses of bi-directional functionally graded truncated conical shells". In: *Mechanics Based Design of Structures and Machines* 48.4 (July 2020), pp. 433–458. ISSN: 15397742. DOI: 10.1080/15397734.2019.1636657.

[3] Herbert Saunders, E. J. Wisniewski, and Paul R. Paslay. "Vibrations of Conical Shells". In: *The Journal of the Acoustical Society of America* 32.6 (June 1960), pp. 765–772. ISSN: 0001-4966. DOI: 10.1121/1.1908207.

[4] Joseph Kempner. *HYMAN GARNET Axisymmetric Free Vibrations of Conical Shells'*. Tech. rep. 1964. URL: http://asmedigitalcollection.asme.org/appliedmechanics/article-pdf/31/3/458/5446138/458_1.pdf.

[5] John E. Goldberg, John L. Bogdanoff, and Lee Marcus. "On the Calculation of the Axisymmetric Modes and Frequencies of Conical Shells". In: *The Journal of the Acoustical Society of America* 32.6 (June 1960), pp. 738–742. ISSN: 0001-4966. DOI: 10.1121/1.1908201.

[6] Guoyong Jin et al. "A modified Fourier series solution for vibration analysis of truncated conical shells with general boundary conditions". In: *Applied Acoustics* 85 (2014), pp. 82–96. ISSN: 1872910X. DOI: 10.1016/j.apacoust.2014.04.007.

[7] Y P Guo. "Normal mode propagation on conical shells". In: *The Journal of the Acoustical Society of America* 96.1 (July 1994), pp. 256–264. ISSN: 0001-4966. DOI: 10.1121/1.410478. URL: https://doi.org/10.1121/1.410478.

[8] Guangjian Ni and Stephen J Elliott. *Wave Interpretation of Numerical Results for the Vibration in Thin Conical Shells*. Tech. rep.

[9] C Shu. *AN EFFICIENT APPROACH FOR FREE VIBRATION ANALYSIS OF CONICAL SHELLS*. Tech. rep. 1996, pp. 935–949.

[10] I S Ran et al. *A CONICAL SHELL FINITE ELEMENT*. Tech. rep., pp. 901–910.

[11] Z. A. B. Ahmad, J. M. Vivar-Perez, and U. Gabbert. "Semi-analytical finite element method for modeling of lamb wave propagation". In: *CEAS Aeronautical Journal* 4.1 (Apr. 2013), pp. 21–33. ISSN: 1869-5582. DOI: 10.1007/s13272-012-0056-6.

[12] Wenbo Duan and Tat Hean Gan. "Investigation of guided wave properties of anisotropic composite laminates using a semi-analytical finite element method". In: *Composites Part B: Engineering* 173 (Sept. 2019). ISSN: 13598368. DOI: 10.1016/j.compositesb.2019.106898.

[13] Pengfei Liu et al. "Application of dynamic analysis in semi-analytical finite element method". In: *Materials* 10.9 (Aug. 2017). ISSN: 19961944. DOI: 10.3390/ma10091010.

[14] "a finite element based on a discrete layer theory for the free vibration analysis of conical shells_Ramesh_Ganesan". In: ().

[15] G B Warburton. *VIBRATION QF THIN CYLINDRICAL SHELLS*. Tech. rep.

[16] Joseph Callahan and Haim Baruhh. *A closed!form solution procedure for circular cylindrical shell vibrations 0*. Tech. rep.

[17] H. R. Ovesy and J. Fazilati. "Stability analysis of composite laminated plate and cylindrical shell structures using semi-analytical finite strip method". In: *Composite Structures* 89.3 (July 2009), pp. 467–474. ISSN: 02638223. DOI: 10.1016/j.compstruct.2008.10.003.

[18] A. Alijani et al. “Development of a semi-analytical nonlinear finite element formulation for cylindrical shells”. In: *Proceedings of the Institution of Mechanical Engineers, Part C: Journal of Mechanical Engineering Science* 228.2 (Feb. 2014), pp. 199–217. ISSN: 09544062. DOI: 10.1177/0954406213486383.

[19] *COMSOL Multiphysics® v. 6.2. www.comsol.com. COMSOL AB, Stockholm, Sweden.*

[20] H. Bagheri, Y. Kiani, and M. R. Eslami. “Free vibration of joined conical-conical shells”. In: *Thin-Walled Structures* 120 (Nov. 2017), pp. 446–457. ISSN: 02638231. DOI: 10.1016/j.tws.2017.06.032.

[21] H. Bagheri, Y. Kiani, and M. R. Eslami. “Free vibration of joined conical–cylindrical–conical shells”. In: *Acta Mechanica* 229.7 (July 2018), pp. 2751–2764. ISSN: 00015970. DOI: 10.1007/s00707-018-2133-3.

[22] T Irie, G Yamada, and Y Muramoto. *FREE VIBRATION OF JOINED CONICAL-CYLINDRICAL SHELLS*. Tech. rep. 1984, pp. 31–39.

[23] Mauro Caresta and Nicole J. Kessissoglou. “Free vibrational characteristics of isotropic coupled cylindrical-conical shells”. In: *Journal of Sound and Vibration* 329.6 (Mar. 2010), pp. 733–751. ISSN: 0022460X. DOI: 10.1016/j.jsv.2009.10.003.

[24] M. Rezaiee-Pajand, Emad Sobhani, and Amir R. Masoodi. “Semi-analytical vibrational analysis of functionally graded carbon nanotubes coupled conical-conical shells”. In: *Thin-Walled Structures* 159 (Feb. 2021). ISSN: 02638231. DOI: 10.1016/j.tws.2020.107272.